CORRELATION OF DURABILITY ASPECTS OF CONCRETE MIXES WITH THE 28 DAYS STRENGTH & ABSORPTION CHARACTERISTICS

A Thesis Submitted

In Partial Fulfillment of the Requirements for

the award of degree of

Master of Engineering (M.E.)

In

Structural Engineering

Submitted by

KAMAL ANAND

(ROLL NO. 801222007)

UNDER THE GUIDANCE OF

Dr. Shweta Goyal

(Assistant Professor)

DEPARTMENT OF CIVIL ENGINEERING

THAPAR UNIVERSITY, PATIALA – 147004

JULY 2014

DECLARATION

I, Kamal Anand, hereby declare that this thesis entitled **"Correlation of durability aspects of concrete mixes with the 28 days strength & absorption characteristics"** is an authentic record of my study carried out as requirements for the award of degree of **Master of Engineering** in **Structural Engineering** in the Civil Engineering Department, Thapar University, Patiala under the supervision of **Dr. Shweta Goyal, Assistant Professor,** Department of Civil Engineering, Thapar University, Patiala during July 2013 to July 2014. This matter embodied in this report has not been submitted in part or full to any other university or institute for the award of any degree.

Date: 15/07/2014

(Kamal Anand)

Roll No. :801222007

CERTIFICATE

This is to certify that above statement made by the student concerned is correct and true to the best of my knowledge and belief.

Dr. Shweta Goyal
Assistant Professor
Department of Civil Engineering
Thapar University, Patiala

Countersigned by

Dr. Naveen Kwatra
Associate Professor & Head
Department of Civil Engineering
Thapar University, Patiala- 147004

Dr. S.K.Mohapatra
Dean of Academic Affairs
Thapar University, Patiala-147004

ACKNOWLEDGMENT

A thesis cannot be completed without the help of many people who contribute directly or indirectly through their constructive criticism in the evolution and preparation of this work. It would not be fair on my part, if I don't say a word of thanks to all those whose sincere advice made this period a real educative, enlightening, pleasurable and memorable one.

First of all, a special debt of gratitude is owned to my supervisor, **Dr. Shweta Goyal, Assistant Professor,** Department of Civil Engineering, Thapar University, Patiala for their gracious efforts and keen pursuits, which has remained as a valuable asset for the successful completion of research work. Her dynamism and diligent enthusiasm has been highly instrumental in keeping my spirit high. Her flawless and forthright suggestion blended with an innate intelligent application has crowned my task a success.

I would like to express my gratitude to **Dr. Naveen Kwatra, Head of department of Civil Engineering**, Thapar University, Patiala for his kind cooperation and encouragement which helped in the completion of work.

I am extremely thankful **to Mr. Ram Simran** for helping me carry out experimental work.

I would also like to thank my parents, brother and my friends for their constant encouragement during the entire course of my thesis work.

Kamal Anand

(801222007)

ABSTRACT

Concrete structures are designed so that they can satisfy requirements regarding safety, serviceability, durability and aesthetics throughout their design service life. Present design procedures regarding compressive strength required by national or international codes are predominantly based on strength principles. The durability aspect is a natural extension of the classical resistance verification where deterioration effects are normally neglected. However judging the durability by 28 days compressive strength might not give appropriate results. This is because durability is related to ingress chloride of chemical from atmosphere inside concrete. It is related more to properties of surface concrete, whereas compressive strength is a bulk concrete property. Thus there is need to relate durability performance both to the compressive strength (CS) & the parameter depicting the property of surface concrete. Initial surface absorption test (ISAT) is one such parameter. In the present work, corrosion is related to CS and ISAT.

One of the major causes of deterioration of reinforced concrete structure is chloride-induced corrosion of the reinforcing steel. The magnitude of the damage is especially large in structures exposed to marine environments. The capacity of the concrete cementitious system to bind chloride ions has an important effect on the corrosion initiation of the steel reinforcement. In the recent years design is related to durability through analysis of resistance to chloride ingress.

In present research work, cubes of size 150 mm x 150 mm x 150 mm and slabs of size 300 mm x 300 mm x 52mm were casted with two types of cement i.e. OPC and PPC, four water-cement ratios i.e. 0.40, 0.45, 0.50, 0.55 and admixed with 4.5% NaCl by weight of cement. Cubes are tested for compressive strength as well as (ISAT) and corrosion density is measured through Linear polarization resistance (LPR) in slabs made with admixed chloride.

Chloride level does not significantly affect the compressive strength of concrete at 28 days age. It is observed that variation in corrosion current density is not systematic with water-cement ratio. Corrosion is more in OPC cement as compared to PPC. Thus blended cement performed well as compared to OPC. However it can be correlated to combination of CS & ISAT. For that model is developed through GP kernel using various parameters of ISAT and compressive strength.

CONTENTS

LIST OF TABLES

LIST OF FIGURES

CHAPTER 1 INTRODUCTION

1.1 GENERAL

Concrete is one of the widely produced materials on the earth, with consumption above billions of tons. As per present scenario concrete is not at all free from severs degradation problems. Apart from design failures, the major significant cause of deterioration and premature failure of reinforced concrete (RC) structures is corrosion of the steel reinforcement. The failure of structures due to reinforcement corrosion does not imply the structural collapse but in many cases, it is manifested by structural serviceability, characterized by concrete cracking and delamination. The concrete cracking and delamination impair not only the appearance of structure but its serviceability also. Thus corrosion is of major importance while considering the durability and safety of concrete structure. These problems have reached alarming proportions in past three decays leading to very high repair cost that goes sometime much above the initial construction cost. In the extreme situations final collapse of structure is noticed.

The corrosion of steel in reinforced concrete structures is a worldwide problem. Due to the large extent of corrosion problem encountered in reinforced concrete structure all over the world, the durability of concrete structures exposed to aggressive environment has become of major importance. In USA, South Africa and Italy, majority of all reinforced concrete structures exposed to see coast, whether directly to action of sea water or to marine atmosphere showed deterioration in relatively short time. In South Africa serious damages in concrete structures constructed in coastal regions was observed. In tempered climatic regions like Europe and North America, deterioration is mainly caused by deicing salts or carbonation. Corrosion of reinforcement is the major cause of deterioration of concrete structures is coastal areas of Arabian Gulf. The environmental and geomorphic conditions particularly the contamination of soil and ground water with chloride and sulfate ions in coastal areas of Arabian Gulf contribute to reduction in service life of concrete structures. In many parts of India, the premature failure occurred in structures exposed to both marine and away from marine atmosphere.

It is estimated that the cost of corrosion related maintenance and repairs for concrete infrastructure in the world is around $100 billion per year. One of the latest estimates from USA states that the cost of damage due to deicing salts alone is between $325 million and $1000 million per year to bridges and car parks. In UK the Department of Transport estimates a total repair cost £616.5 million ($1200 million) due to the damage caused by corrosion to motorway bridges and these bridges represent about 10% of the total bridge inventory in UK. Therefore the total repair cost may be ten times the Department of Transport estimate. India has a large coastal belt where the corrosion is extremely severe. The cost of corrosion in India is estimated to be around 3,60,000 million rupees ($8 billion) as published in Financial Express. The reinforcement corrosion in concrete is an electrochemical process. In well made and good quality concrete the risk of corrosion is minimal as it normally provides good chemical and physical protection to the embedded steel reinforcement. The chemical protection is through the formation of a passive layer (thin protective oxide film) over the steel surface due to high alkalinity of concrete pore solution while the physical protection is through the retarding access of oxygen, moisture, and various aggressive species to steel/concrete interface. However the breakdown of the passive film and consequently corrosion initiation takes place either when sufficient chloride ions have reached the rebar level or when the pH of the concrete pore solution drops to low values due to carbonation. Chloride ions are considered to be the primary cause of rebar corrosion in concrete, outweighing that due to carbonation. The aggressive chloride ions can be originated either from the use of contaminated mix ingredients at the fresh state or from the surrounding environment in hardened state. The behavior of steel reinforcement varies significantly in concrete containing internal chloride from that exposed to external chloride.

Service life of RC structures exposed to aggressive agents such as chlorides ions consists of two phases namely initiation phase and propagation phase. During initiation phase, initially the steel reinforcement remains passive, however at the end of initiation phase when sufficient amount of chloride ions reach the steel/concrete interface, corrosion initiation takes place. This chloride content is generally known as the critical chloride content. During propagation phase, corrosion once initiated progresses and reaches a level that causes significant damage i.e. reaches serviceability limit.

The addition of alternative materials such as fly ash, ground granulated blast furnace slag, silica fume etc. are known to enhance the durability of reinforced concrete structures. It has been reported that the concrete containing these alternative materials perform excellently in marine environment.

1.2 SCOPE AND OBJECTIVES OF THE PRESENT RESEARCH WORK

A comprehensive discussion regarding rebar corrosion carried out for the research work is presented in Chapter 2 and from the review; it is observed that chloride ions are the dominant cause of rebar corrosion in RC structures. The critical chloride content responsible for initiation of rebar corrosion is not a single value. From the data available in literature, it is found that there is a large scatter in critical chloride value itself. One of the reasons for the uncertainty in the critical chloride content is its dependency on various factors including steel and cement type. The other reason is the lack of accordance on the determining parameters indicating corrosion initiation and on the expression of critical chloride itself as well. Therefore there is a need for identifying the parameter(s) which will serve as the stable indicator of rebar corrosion initiation. This indicating parameter for corrosion initiation shall account for steel surface condition and/ or steel type in addition to accounting for concrete characteristics and the chloride ion concentration.

Further from literature review it is observed that, although some works on determining parameters and critical chloride content leading to initiation of chloride induced corrosion using different types of cement have been carried out by past researchers, work on above parameters using different types of steel is scanty.

Keeping in view the research need identified from the literature review, the objectives of the present research work are formulated as follows;

1. To evaluate the performance of different type of cement against internal chloride exposure through corrosion rate measurement by electrochemical technique (linear polarization resistance) and comparing the same.

2. To relate the performance of concrete in terms of corrosion with compressive strength and initial absorption test (ISAT).

3. To develop the model relating corrosion with compressive strength and ISAT using GP kerenel.

1.3 FORMAT OF THESIS

The thesis has been organized in five chapters:

- In the first chapter the scope and objectives of the research work has been presented.
- In the second chapter, a comprehensive discussion regarding rebar corrosion and genetic programming are presented.
- In the third chapter, review of literature is discussed.
- In the fourth chapter, the experimental investigation for determination of corrosion rate by LPR with internal chloride is carried out. In addition initial surface absorption test is carried out and their compressive strength is compared.
- In fifth chapter results and discussion is presented.
- In sixth chapter conclusion and suggestions for further work are presented.

CHAPTER 2 REBAR CORROSION & GENETIC PROGRAMMING

2.1 GENERAL

Concrete generally provides high degree of protection to the steel reinforcement against corrosion, by virtue of its highly alkaline environment. In addition, well compacted and properly cured concrete with low water-cement ratio has low permeability which reduces the penetration of corrosion agents such as chloride ions, carbon dioxide etc.

In this chapter a thorough comprehensive discussion on corrosion process which emphasis on rebar corrosion is presented, it is observed that chloride induced reinforcement corrosion is the most frequently occurring durability problem encountered in RC structures as compared to other causes such as carbonation etc. Therefore, in this context, past research work on chloride induced rebar corrosion is further described whereby critical conditions leading to rebar corrosion initiation is discussed. Followed by the above discussion, work carried out by past researchers on cement type on chloride induced corrosion is presented. Then a brief discussion on various corrosion tests used for corrosion investigation in reinforced concrete is presented. Lastly the summary and inferences drawn from review of literature are presented.

2.2 CORROSION PROCESS WITH EMPHASIS ON REBAR CORROSION

Corrosion is defined as the undesirable deterioration of a metal or alloys i.e. an interaction of the metal with its environment that adversely affects those properties of the metal that are to be preserved *(Shreir, L.L., 1976)***.**

The corrosion processes can be classified into two types namely wet corrosion process and dry corrosion process (*Shreir, L.L., 1976*). The wet corrosion process includes all reactions in which water or an aqueous solution is involved in the reaction mechanism while dry corrosion process includes reactions in the absence of water or an aqueous solution. Since the rebar corrosion involves metal dissolution in aqueous media, it is a

wet corrosion process and it is established that this is an electrochemical process involving charge transfer.

2.2.1 Rebar Corrosion: An Electrochemical Process

The electrochemical processes require anodes and cathodes in electrical contact as well as an ionic conduction path through an electrolyte. The corrosion of steel in concrete is considered as an electrochemical process with anodes and cathodes formed adjacently on the rebar and are surrounded by the concrete pore solution which acts as the electrolyte allowing the movement of ions between anodic and cathodic sites.

This electrochemical process involves following reactions;

a) Oxidation of iron at anode liberates electrons and gives rise to the formation of iron ions [$Fe \rightarrow Fe^{2+} + 2e^-$] whose hydrolysis produces acidity [$Fe^{2+} + 2H_2O \rightarrow Fe(OH)_2 + 2H^+$]

b) Reduction of oxygen at cathode that consumes these electrons and produces alkalinity [$O_2 + 2H_2O + 4e^- \rightarrow 4(OH)^-$]

c) Transport of electrons within the metal from the anodic regions to cathodic regions where they are consumed and since the electrons carry a negative charge, this results in the flow of electrical current in opposite direction.

d) Finally in order that the circuit to be complete, the flow of current inside the concrete from anodic regions to cathodic regions takes place through transport of ions in the concrete pore solution.

These four processes are complementary and they occur at the same rate. The flow of electrons between the anodic and cathodic areas quantifies the rates of oxidation and reduction reactions. The anodic current I_a i.e. number of electrons liberated by the anodic reaction, cathodic current I_c i.e. the number of electrons consumed in the cathodic reaction, the current that flows within the metal i.e. steel reinforcement from cathodic region to anodic region (I_m) and lastly the current that flows inside the concrete from anodic region to cathodic region (I_{con}) must be equal *(Bertolini et al. , 2004)*. A schematic representation of the rebar corrosion process is shown in Fig. 2.1.

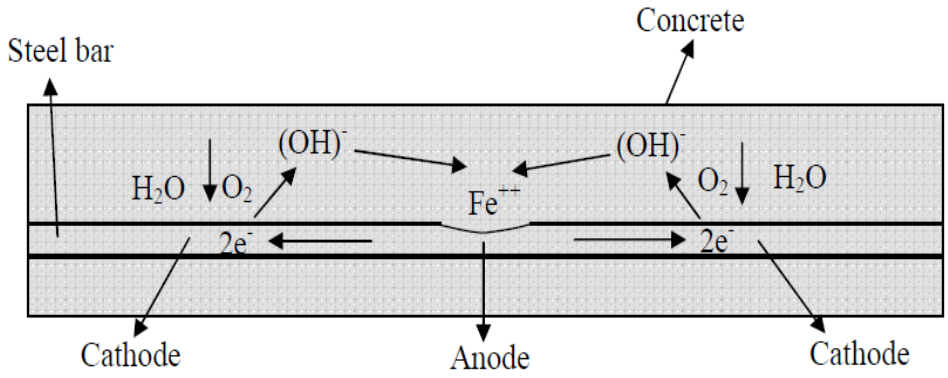

Fig. 2.1: Schematic representation of electrochemical rebars corrosion process

However the corrosion rate is negligible when one of the following conditions exists.

(i) Anodic process becomes slow because when the concrete is not carbonated and does not contain chlorides, it results in steel reinforcement to remain passive. This is referred as passive control.

(ii) Cathodic process is slow. This is because the rate at which oxygen reaches the steel surface is low, as in case of water saturated concrete. This is referred as control of oxygen transport.

(iii) Electrical resistance of the concrete is high, as in case of structures exposed to environments which are dry or low in relative humidity. This is referred as Ohmic control.

According to the different spatial locations of anode and cathode, corrosion of steel in concrete can occur in different forms namely microcell and macrocell. Microcell corrosion occurs when anodic dissolution reaction and cathodic reduction reaction take place adjacently to each other on the same steel bar. On the other hand macrocell corrosion occurs when actively corroding steel bar is coupled to another steel bar which is either passive or corroding at a lower rate, because of its different composition or different environment *(Hansson et al., 2006).* Macrocell can also occur on the same steel bar exposed to different environments within the concrete itself or when part of the steel bar extends outside the concrete.

Although the corrosion rate may be negligible when one of the above stated conditions exist, the tendency to corrode is inherent to steel and will always exist. To

understand the corrosion tendency, one may adopt the thermodynamic approach and the same is presented in the next section.

2.3 CORROSION TENDENCY: A THERMODYNAMIC APPROACH

The tendency of a particular metal to participate in an electrochemical reaction in a particular environment can be viewed thoroughly and completely from the standpoint of chemical thermodynamics. The tendency for any chemical reaction to proceed, including the reaction of a metal with its environment, is measured by the Gibbs free energy change ΔG *(Shreir, L.L., 1976)*. The magnitude of ΔG, of a specific corrosion reaction provides a measure of spontaneity of the reaction and of the extent to which it will proceed before equilibrium is attained. The more negative the value of ΔG, the greater is the tendency for the reaction to proceed, however the rate and extent of reaction depend on kinetic factors which control the rate of reaction leading to final position of equilibrium. Thus the tendency to corrode is not a measure of the reaction rate. A large negative value of ΔG may or may not be accompanied by a high corrosion rate, but when ΔG is positive it can be stated that the reaction will not proceed at all. When ΔG = 0, a condition of equilibrium is attained. In view of the electrochemical mechanism of corrosion, the tendency for a metal to corrode can also be expressed in terms of the electromotive force (emf) of the corrosion cells that are an integral part of the corrosion process.

2.3.1 Free Energy Change and Rate of Reaction

Considering the following chemical reaction;

$$aA + bB \longrightarrow cC + dD \qquad (2.1)$$

Where A is the metal, B is a reactant in the solution and C and D are reaction products as shown in Fig. 2.2 (a, b, c, d) are the corresponding number of moles of the reactants and products. -ΔG is the decrease in free energy change. It shows that although the thermodynamic tendency is same for L, M, and N the rates at which the final equilibrium position is reached are different. An analogy can be drawn between above situation and corrosion process by considering L as a steel reinforcement embedded in a chloride contaminated poor concrete, M, the steel reinforcement protected by epoxy coating, and N, the steel reinforcement coated with epoxy and also cathodically protected. In each case the free energy change for the corrosion reaction

is the same but the rate at which the reaction proceeds to equilibrium varies significantly. More negative value of ΔG indicates higher tendency of the above reaction to proceed from left to right.

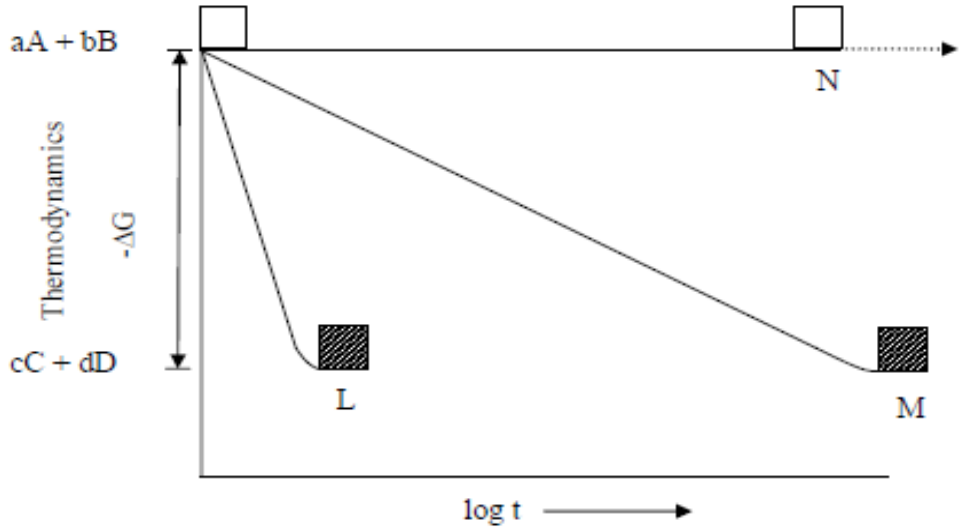

Fig. 2.2: Relationship between thermodynamic tendency and rate of reaction,

(Shreir, L.L., 1976)

2.3.2 Free energy change and electrode potential

For the chemical reaction (2.1), the free energy change ΔG which accompanies the transformation of molar quantities of reactants to products is given by the following expression;

$$\Delta G = \Delta G^{\circ} + RT\ ln\frac{[C]^c[D]^d}{[A]^a[B]^b} \qquad (2.2)$$

Where R is gas constant

T = absolute temperature

ΔG°= standard free energy change

An electrochemical reaction involving transfer of electrons may be represented as;

$aA + bB + ne^- \rightarrow cC + dD$ (2.3)

Corresponding free energy change ΔG is related to the electrode potential E by the fundamental relationship;

$$\Delta G = -nFE \quad (2.4)$$

Where n is the number of electrons (or equivalents) exchanged in the reaction, and F is the Faraday's constant, 96500 coulombs.

Substituting ΔG = -nFE and ΔG° = -nFE° in equation (2.2), the electrode potential E is given by;

$$E = E^0 + \frac{RT}{nF} ln \frac{[A]^a[B]^b}{[C]^c[D]^d} \quad (2.5)$$

Equation (2.5) is the common form of Nernst equation. Here E^0 is the standard electrode potential for the reaction. By knowing the value of standard electrode potential for a particular electrochemical reaction, it is possible to predict the range of electrode potentials over which the reaction will be thermodynamically possible at any given combination of concentrations of the reactants and products. Thus potential difference (voltage) is the driving force for an electrochemical reaction. Electrode potential represents the potential difference between the electrode (steel) and the adjacent electrolyte (concrete). This electrochemical potential is a measure of the ease of electron charge transfer between the steel and the concrete pore water solution and is thus a property of the steel/concrete interface and is a measure of thermodynamic tendency of metal dissolution *(Schiessel, P., 1988)*. The electrode potential is always lower at a local anode than at a cathode of the corrosion couple. The difference in electrode potentials at anode and cathode (i.e. electrode potential at cathode - electrode potential at anode) may be very small if they are closely spaced and the electrolyte is of high conductivity. However the difference may be of the order of several hundred milli volts if the anodes and cathodes are separated by a medium of high resistance.

2.4 INTRODUCTION TO GENETIC PROGRAMMING

Genetic Programming is a technique for the automatic and systematic solving of problems by means of algorithmic evolution, regardless of domain. This is why it is a good candidate for the solving of the feature selection and construction problem for

image classification which often suffers from domain specificity and bloated numbers of features. Just as in many domains it has matched or exceeded human intuition and engineering, even creating patentable solution in some cases, it has the potential to improve on the classification performance of the hand crafted Haralick features and features like them.

2.4.1 The GP algorithm

The basic idea of Genetic Programming is to stochastically create and then transform a population of programs, a generation at a time, into better and better solutions for the problem at hand. This is done by, at every generation, evaluating the fitness of the population and then using genetic operators to push and build the changing population of programs towards better and better solutions. The idea is that we do not know exactly how to make these good solutions but we do have methods for judging and measuring the goodness of solutions that the stochastic evolutionary process produces. The principle of survival of the fittest and the genetic operators ensure that when good solutions are found, they propagate in the population and eventually are even built on top of to produce better solutions down the road. What the "programs" are which are being evolved just depends on the domain. For feature construction, we are evolving The Genetic Programming algorithm is basically: randomly generate a population of valid programs, execute each program and measure its fitness, select some individuals with a probability based on fitness scores to participate in genetic operations, and apply the operators to the individuals to create a new generation of individuals. This process begins again with the calculating of the fitness scores of the new population of solutions and repeated until an optimal solution is found or some other stopping condition is met. The end result is the returning of the best individual found. In order to accomplish this whole process, methods need to be established for the representation of programs, the evaluation of fitness, the selection of individuals from the population, and the execution of genetic operators.

2.4.2 GP kernel steps

1.) Create the data file and save in the same directory as the program (e.g. *C:\project\project1.csv*)

2.) Since there will be so far no proper directory structure we have to run

gpkernel *project1****.ini ini2dir***

This will create the general ini file (e.g. *project1*.*ini*), as well as the folders and subfolders containing the necessary files.

3.) In the dataSource subfolder we change **sourcefile** i.e. at the file *C:\project\d2k.$$$\project1.d2k****dataSource\data.ini,*** we change **sourcefile=**project1.csv

4.) Run ***gpkernel*** *project1****.ini fromdir***

the parameter ***fromdir*** is used because we have changes within the structure directory that we want to be reflexed both on the ini file and on the rest of the subdirectory structure.

5.) In the dataSource subfolder change (in the ***data.ini*** file again) other parameters such as the existence of headers, delimiter, size of the training set, …

6.) Run

gpkernel *project1****.ini fromdir***

7.) If adding dimension information, change in the file C:\project\d2k.$$$\project1.d2k**Dimension\data.ini** the item **NumberOfItems=_** to the number of magnitudes dimensions.

8.) Run

gpkernel *project1****.ini fromdir***

This will create subfolder for all the dimensions, in each subfolder

…**Dimension\Dimension**x

change the **data.ini** file:

dimensionName=Length

dimAbbreviated=L

unitName=meter

unitAbbreviated=m

9.) Run

gpkernel *project1****.ini fromdir***

This will affect the information contained for the different **Inputs**, **Targets**, and **Constants** information, that will be created next.

10.) Change in the ***…\dataSource\inputs\data.ini*** file

NumberOfItems=__

gpkernel *project1****.ini fromdir***

Then we will have created the subfolders for the different input sets.

11.) For each Inputs_, change the name, location in the source file (0, 1, …), and dimensions (if necessary)

gpkernel *project1****.ini fromdir***

12.) Do the same for the target field (10. and 11.)

13.) Proceed analogously with the constants

14.) The general **ini** file should show in the section **[dataSource]** the line

status=done

This means that the data source is properly setup.

15.) Change in the pool subdirectory the value of

NumberOfItems=*1* (e.g.)

(*) *see step 17*

gpkernel *project1****.ini fromdir***

Then the following message appears:

Pool0 is not ready yet. Check parameters and status.

16.) For each pool we set:

- 13. A.) Objective: number, ***gpkernel*** *project1****.ini fromdir***

  In each objective we can set:

  objectivetype= CoD / RMS

- 13. b.) Change the ini file in …\lTable
- 13. c.) Change the Evolution Parameters

  gpkernel *project1****.ini fromdir***

We get the message:

All pools are setup properly. You can now set the

"Run experiments On Startup" variable on true

17.) Optionally, change **TimeOut=_** , and **Number of Experiments**= _ in

…\pool\data.ini , ***gpkernel*** *project1****.ini fromdir***

(*) This step number 17 can also be done at the same time as step 15.

18.) In the **…***project1***.d2k\data.ini*** file set "Run experiments On Startup" variable on true,

gpkernel *project1****.ini fromdir***

The program should now start running.

2.4.3 Advantages of Genetic Programming

A key advantage of GP when compared to traditional modelling approaches is that it does not assume a prior functional form of the solution. For instance, in a typical regression method, the model structure is specified in advance (which is in general difficult to do) and the model coefficients are determined. For neural networks, the time consuming task of initially defining the network structure has to be undertaken and then the coefficients (weights) are found by the learning algorithm. On the other hand, in GP, the building blocks (the input and target variables and the function set) are defined initially, and the learning method subsequently finds both the optimal

structure of the model and its coefficients. Moreover, since GP evolves an equation or formula relating to the input and output variables, a major advantage of the GP approach is its automatic ability to select input variables that contribute beneficially to the model and disregard those that do not. GP can thus reduce substantially the dimensionality of the input variables. However, a common limitation of GP is that it cannot handle more numbers of constants. In GP, as in any data-driven prediction model, the selection of appropriate model input is extremely important. Inclusion of irrelevant input parameters leads to poor model accuracy and creation of complex models, which are more difficult to interpret as compared to simpler ones.

2.5 CLOSING REMARKS

The comprehensive discussion on rebar corrosion and genetic programming has been described in this chapter. Various approaches of rebar corrosion are discussed and various steps involved in this genetic programming are described.

CHAPTER 3 LITERATURE REVIEW

3.1 GENERAL

The corrosion of the steel reinforcement embedded in concrete is most frequently the result of the chloride included breakdown of the passive film formed in the high alkaline environment of the concrete. It has been reported in past that the corrosion initiation takes place when the chloride concentration at the rebar level reaches a critical value. It is also reported that the above critical chloride concentration level is an important parameter in determining the durability-life and /or service-life of reinforced concrete structures. The critical chloride level to develop active corrosion of the steel reinforcement is unlikely to be a unique value. It depends upon various factors such as C_3A content of the cement, blended materials, chloride binding, concrete mix proportions, w/c ratio, concentration of hydroxyl ions, temperature, relative humidity, source of chloride and also on cement type and steel type. Out of the above factors most easily controllable parameters are concrete mix proportion, cement type.

3.2 EFFECT OF CEMENT TYPE ON CRITICAL CHLORIDE LEVELS IN CONCRETE

Oh et al. (2003) have measured half-cell potential values and extent of corroded area of steel specimens in prismatic concrete specimens and determined the threshold free chloride, total chloride and $[Cl^-/OH^-]$ ratio in the concrete specimens made with OPC (Type I cement) , SRPC (sulfate-resisting Portland cement) i.e. Type V cement, OPC with fly ash and OPC with slag. Chloride was admixed into concrete as sodium chloride of which the concentrations varied from 0 – 2% by weight of binder. The concrete mixture made with SRPC exhibited relatively more negative values of halfcell potentials at the same total chloride content as compared to other mixtures and also the bars embedded in concrete with SRPC showed a relatively higher corrosion area at the same chloride content. The chloride threshold values were determined corresponding to half-cell potential value of -300mV ($Cu/CuSO_4$ reference electrode) at which the extent of corroded area of the steel reinforcement increased significantly. The threshold values of free chloride and total chloride contents for different types of cement were in the range of 0.07% – 0.13% and 0.45%

- 0.97% by weight of the cement respectively. The authors are of the opinion that, as the range of the threshold values of free chloride content is much less than that of total chloride content, the free chloride values are more reliable for specifying a limiting value for corrosion initiation in reinforced concrete structures. It was found that the sulfate resisting Portland cement exhibited more amount of free chloride concentration at the same amount of total chloride addition than ordinary Portland cement. This was due to lower chloride binding capacity of SRPC as compared to that of OPC. The threshold value of the total chloride decreased with an increase in the fly ash content and this effect results from the decrease of the pH value by addition of fly ash. The threshold values of $[Cl^-/OH^-]$ ratio were in the range of 0.16 – 0.26, depending upon the cement type.

Hussain et al. (1996) have carried out half-cell potential measurement on prismatic mortar specimens immersed partially in 5% NaCl solution. The specimens were made with three Portland cements with different C_3A contents and with a centrally embedded steel bar. A half-cell potential of -270mV with reference to saturated calomel electrode (SCE) was taken as the threshold potential for corrosion initiation. After the above threshold potential is reached the specimens were taken out of the chloride solution and the pore solution was analyzed for Cl^- and OH^- concentrations. From the results the authors observed hat, corrosion initiation time of steel depends upon the C3A content of the cement and it increases with an increase in C_3A content. The threshold $[Cl^-/OH^-]$ ratio seemed to depend on the pore solution pH and was found to vary from 1.28 to 2.0 for a pore solution pH of 13.26 to 13.36. The threshold value of free chloride content varied from 0.22% to 0.29% by weight of cement and was independent of the C_3A content of cement. However, the threshold total chloride contents were dependent on the C_3A content of the cement and varied from 0.48% to 0.59%, 0.73% to 0.85%, and 1.01% to 1.20% by weight of cement for 2.43%, 7.59%, and 14% C_3A cements respectively.

Thomas (1996) has carried out an experimental investigation to study the marine performance of fly ash concrete. The reinforced concrete specimens of different strength grades were made with OPC and varying levels of fly ash and exposed to tidal environment for determination of the threshold chloride content. After exposure periods of 1, 2, and 4 years the specimens were retrieved for chloride content analysis

and measurement of steel mass loss. From the results the author observed that the steel mass loss increased with chloride content and presented the relationship between the steel mass loss and chloride concentration at the level of steel. The threshold value of the acid soluble chloride content decreased with increase in fly ash content. The values obtained were 0.7%, 0.65%, 0.5%, and 0.2% by mass of cement for concrete with 0%, 15%, 30%, and 50% fly ash, respectively. The lower threshold values of total chloride are probably a corollary of higher [Cl^-/OH^-] ratio in the pore solution of fly ash concrete compared with OPC concrete of the same total chloride content. Despite the lower threshold levels, lower steel mass loses were observed with higher fly ash levels as they provided better protection to the steel reinforcement and this is clearly attributed to the increased resistance of fly ash concrete to chloride ion penetration.

Chalee et al. (2007) et al. have carried out an experimental investigation to study the effect of w/c ratio, fly ash replacement on cover depth against corrosion of steel embedded in OPC and fly ash concrete in marine environment up to 4 years. Different percentages of fly ash used as partial replacement were 15%, 25%, 35% and 50% by weight of cementitious material. The water to cementitious materials ratios of fly ash concretes used were 0.45, 0.55, and 0.65. The specimens were tested for compressive strength, chloride penetration profile and corrosion of the embedded steel bar after exposed to tidal zone of marine environment in Gulf of Thailand for periods of 2, 3, and 4 years. From the results obtained, it was noted that chloride penetration of fly ash concrete was lower than that of OPC concrete and decreased with increase in fly ash content. The threshold chloride content required to initiate the corrosion of the embedded steel reinforcement was determined corresponding to about 1-2% rusted area. The fly ash concretes resulted in lower values of chloride threshold than that of controlled concrete for all water to cementitious materials ratios at all ages and threshold chloride content decreased with increase in fly ash content. Increase in fly ash content and decrease in water to cementitious materials ratio could reduce the cover depth required for initial corrosion of the steel reinforcement.

3.3 EFFECT OF STEEL TYPE ON CRITICAL CHLORIDE LEVELS IN CONCRETE

Bhattacharjee et al. (1995) has carried corrosion study on reinforced concrete beams, 150cm long with 10 x 20 cm^2 cross-section were cast. The concrete used was w/c ratio of 0.64 and three different concentrations of $CaCl_2$, namely 0%, 1% and 2.5% by mass of cement used as corrosion inducing admixture. Each beam had two twisted steel reinforcing bars (grade –HY420), 1.2 cm in diameter and 145 cm in length embedded in concrete and 5cm for electrical connections. The results observed show that corrosion is uniform over the entire length of reinforcing bar and values of E_{corr}, I_{corr} , B etc., measured at eight points on the beam did not demonstrate considerable variation except for one or two points on beam. This was expected as $CaCl_2$ was mixed uniformly throughout the concrete.

Trejo and Pillai (2003) have presented an accelerated standard methodology to evaluate the critical chloride threshold value of two different types of steel reinforcement embedded in mortar samples made with ordinary Portland cement. From the results of accelerated chloride threshold (ACT) test, the authors found that, ASTM A615 steel reinforcement in the mortar specimen exhibited a mean critical chloride threshold value of 0.52 kg/m^3 with the range from 0.30 to 0.71 kg/m^3 at 95% confidence level. On the other hand ASTM A706 reinforcing steel exhibited a mean critical chloride threshold value of 0.20 kg/m^3 with the range from 0.15 to 0.24 kg/m^3 at 95% confidence level.

Trejo and Monteiro (2005) have carried out an experimental investigation to determine the critical chloride threshold, macrocell corrosion rate and mass loss for ASTM A706 and ASTM A615 reinforcing steel specimens embedded in concrete and mortar specimens made with OPC and exposed to chloride solution. The critical chloride threshold values for the two types of steel reinforcement embedded in mortar specimens were determined by accelerated chloride threshold (ACT) test method while the southern exposure (SE) concrete samples were used to determine the macrocell corrosion rate and mass loss of the above two types of steel reinforcement. ASTM A706 steel exhibited lower values critical chloride threshold than ASTM A615. The average critical chloride threshold values exhibited by ASTM A706 and ASTM A615 were 0.19 kg/m^3 and 0.87kg/m^3 respectively. In addition the average

corrosion rate of SE samples embedded with ASTM A706 steel was approximately 68% higher than that exhibited by SE samples embedded with ASTM A615 steel. Thus ASTM A706 steel was more susceptible to chloride induced corrosion than ASTM A615 steel.

Alonso et al. (2000) have carried out chloride threshold studies based on corrosion rate measurements in mortar specimens admixed with various percentages of sodium chloride and calcium chloride and embedded with steel reinforcement. Two types of steel reinforcement with different surface condition i.e. one with ribbed and other with smoothed surface was used. The composition of the two steel bars was kept identical. The sodium chloride content varied from 0.79% to 5.14% by weight of cement and calcium chloride content was 5.38% by weight of cement. Active corrosion was considered, when the corrosion rate of the rebar in a small exposed area was higher than $0.1\mu A/cm^2$. The corrosion potential (E_{corr}), polarization resistance (R_p) and the electrical resistance were measured periodically and I_{corr} was calculated using Stern-Geary equation. At the end of the experiment, by visual observation, it was found that the specimens having I_{corr} values above $0.1\mu A/cm^2$ showed visible corrosion. The threshold total chloride content varied from 1.24% to 3.08% by weight of cement and the threshold free chloride content was in the range from 0.39% to 1.16% by weight of cement. The threshold $[Cl^-/OH^-]$ ratio varied from 1.17 to 3.98. The effect of steel type on chloride threshold was not significant; however the ribbed bars showed a bit higher susceptibility to corrosion with the mean I_{corr} was slightly higher than the smoothed bars.

Trejo (2002) has undertaken a study to evaluate the critical chloride threshold and corrosion rate of different types of steel reinforcement by carrying out ACT test methodology and macrocell test methodology. ACT test was used to determine the critical chloride threshold of steel reinforcement while ASTM G109 test method was used to evaluate the macrocell corrosion current between top and bottom steel. The different steel reinforcements used were ASTM A615, ASTM A706, 304 stainless steel, 316LN stainless steel and a microcomposite steel reinforcement. From the results the author observed that the critical chloride threshold values for ASTM A615 steel, microcomposite steel and 304 stainless steel are $1.1lb/yd^3$, $8.3lb/yd^3$, and $8.4lb/yd^3$ of concrete. The results for ASTM A706 and 316LN stainless steel are not available.

3.4 AMBIGUITY IN CRITICAL LEVELS FOR CORROSION INITIATION/DEPASSIVATION

The dependency of the critical chloride level, which is also often referred as the threshold chloride concentration, on large number of variables as mentioned earlier is the reason for its ambiguity and uncertainty. Therefore expressing a unique value of critical chloride for all types of cement, steel, and mix parameters etc. as an indicator of corrosion initiation can be misleading. The other reason is the lack of accordance for the definition of the chloride threshold itself either on the determining parameters i.e. corrosion current, corrosion potential or visual observation, or on the expression of threshold such as [Cl^-/OH^-] ratio, concentration of free or total chloride etc.

Alonso et al. (2000) have presented the critical thresholds reported by various authors for depassivation of steel reinforcement. From these reported values, it is observed that, the researchers have reported the chloride threshold in different forms i.e. free chloride, total chloride and/or [Cl^-/OH^-] ratio. Also it is noted there is a large scatter in the values of critical chloride levels itself and the depassivation detection techniques used by them are also different. Glass and Buenfeld have published an interesting discussion on the chloride threshold level presented by various authors in different conditions: namely outdoor concrete structures and laboratory experiments using concrete, mortar, paste and solutions. From the review, it was shown that the value of total chloride content expressed as percentage by mass cement is in the range of 0.17 - 2.5, thus the highest value is about 15 times the lowest value in the range. These remarkable differences clearly illustrate the difficulty in establishing such parameter.

In addition to the different values of critical chloride reported by various researchers, different standards have also set different values for maximum limit of chloride content. A value of 0.4% by mass of cement has been specified by the British Standard BS 8110 as the maximum limit for total chloride content. ACI 318 specifies a water soluble chloride content of 0.15% of the mass of cement while ACI 222 specifies acid soluble chloride content of 0.20% by mass of cement. The limit set by Australian standards is 0.8 kg/m^3 of concrete which works out to be 0.235% by mass of cement for a typical concrete. As per Indian standards IS 456 - 2000, the maximum allowable acid soluble chloride content for reinforced concrete containing embedded metal is 0.6 kg/m3 of concrete.

Hausmann was the first to identify the threshold value of [Cl^-/OH^-] ratio, as 0.6 in simulated concrete pore solution. According to Alonso et al. the [Cl^-/OH^-] ratio seems to be the most accurate parameter for defining the threshold value for depassivation while evaluating corrosion onset on reinforced concrete. However, due to the difficulty involved in measuring the OH^- concentration in concrete, the free and total chloride content by mass of cement or concrete are the other parameters those have been widely used to represent the critical chloride indicating the risk of corrosion. The authors [22] observed that for steel in concrete slabs exposed to external sources of chloride, the critical value of [Cl^-/OH^-] ratio necessary for depassivation of reinforcing steel was approximately 3 which is more than the value of 0.6 suggested by Hausmann.

According ASTM C 876 criteria, the potentials more negative than -350mV($Cu/CuSO_4$ reference electrode)/-270mV(SCE) over an area correspond to 90% or greater probability of occurrence of corrosion of steel reinforcement in that area. Hussain et al. have adopted the half-cell potential value of -270mV (SCE) as the threshold potential for onset of corrosion. Oh et al. have determined the chloride threshold values corresponding to half-cell potential value of -300mV($Cu/CuSO_4$ reference electrode) at which the extent of corroded area of the steel reinforcement increased significantly. Soleymani and Ismail have presented threshold values of corrosion current density measured through linear polarization resistance (LPR) and Tafel plot (TP) techniques and the corresponding corrosion activity levels. According to the criterion, if the value of corrosion current density is less than $0.2\mu A/cm^2$, then corrosion rate is negligible and steel reinforcement is in passive state. When the value of corrosion current density is between $0.2\mu A/cm^2$ and $1\mu A/cm^2$, then corrosion has initiated and is proceeding at a moderate rate. If the value of corrosion current density is greater than $1\mu A/cm^2$, then corrosion rate is high. In addition to that Soleymani and Ismail have also presented the corresponding values of free chloride content and half-cell potential (HCP) for the above corrosion activity levels. Further, they observed that the above four testing methods (LPR, TP, chloride content, HCP) predicted the same corrosion activity level for only 24% of the total specimens tested. In those cases where the specimens had different corrosion activity levels, chloride content method estimated lowest corrosion activity level, while the TP and LPR methods estimated highest corrosion activity levels. On the other hand HCP method estimated

an intermediate corrosion activity level amongst the other methods. The criterion of $0.2\mu A/cm^2$ corrosion rate as the critical level for active corrosion initiation has been adopted by other researchers as well.

Erdogdu et al. (2001) on the basis of the measured values of corrosion current density have given criteria for corrosion activity. Corrosion current density values less than $0.1\mu A/cm^2$ correspond to passive condition and corrosion current density values ranging between $0.1\mu A/cm^2$ and $1\mu A/cm^2$ correspond to moderate corrosion rate. Similarly corrosion current density values ranging between $1\mu A/cm^2$ and $10\mu A/cm^2$ and between $10\mu A/cm^2$ and $100\mu A/cm^2$ correspond to high and very high corrosion rate respectively. Other researchers have stated that, depassivation is considered when the value of corrosion current density is greater than $0.1\mu A/cm^2$.

3.5 PERFORMANCE OF CEMENT AND STEEL TYPE AGAINST CHLORIDE INDUCED CORROSION

In addition to the work on critical chloride level for corrosion initiation, some other works have been carried out by past researchers on the performance of different types of cement and steel against chloride induced corrosion and are presented here.

3.5.1 Performance of cement type

Basheer et al. (2002) have monitored the continuous behaviour of slab specimens made with concrete mixes containing alternative cementitious materials (ACMs) such as pulverized fuel ash (PFA), ground granulated blast furnace slag (GGBS), microsilica (MS) and metakaolin (MK) subjected to a cyclic ponding regime with 0.55M sodium chloride solution for one year. The changes in concrete were monitored by measuring the changes in the resistance between the pairs of stainless steel electrodes embedded at different depths from the exposed surface of the slab specimens and it has been found that although the resistance of concrete decreased initially due to the penetration of chlorides, in the long term the resistance of the concrete mixes containing ACMs performed better than controlled concrete made with OPC.

Lambert et al. (1991) have carried out an experimental investigation in both internal and external chloride exposure on concrete slab specimens made with OPC and SRPC and mild steel rods. For internal chloride exposure, the slabs were admixed with

sodium chloride and added at levels of 0.4%, 1%, and 2% chloride ion by weigh of cement. For slabs prepared without internal chloride additions, were exposed to 5% sodium chloride solutions up to two years under the conditions such as constantly maintained solution, weekly wet/dry cycle, and monthly wet/dry cycle. The corrosion potential (E_{corr}) and polarization resistance (R_p) were determined at regular intervals and the corrosion rates were calculated from the measured values of R_p using the Stern-Geary equation. After the completion of the exposure test, they have measured the weight loss gravimetrically due to corrosion of the bars after removing them from the slabs. From the results the ranking of materials and exposure regimes with regard to corrosion severity was carried out. The steel in concrete containing internal chloride exhibited higher corrosion rates at relatively lower [Cl^-/OH^-] ratio as compared to that exposed to external chloride solution. This is because when the reinforcing steel is embedded in concrete containing internal chloride, it comes in contact with the aggressive chloride-rich medium right from the moment of casting before the formation of an effective passive film and a surrounding lime-rich zone of hydration products. On the other hand the steel reinforcement embedded in concrete exposed to external chloride source would have been surrounded by a passivating alkaline environment for a substantial period before it comes in contact with the chloride ions.

Dhir et al. (1994) have undertaken an experimental investigation to determine effect of pulverized fuel ash (PFA) on rebar corrosion due to both admixed chloride (internal) and external chloride by measurement of half-cell potential and polarization resistance (R_p) at regular intervals over the exposure period and water soluble chloride in concrete specimens made with OPC and OPC with different proportions of PFA. The corrosion current density was calculated using polarization resistance from Stern-Geary equation. From the results it was observed that for specimens made with admixed chloride, the water-soluble chloride content in PFA was always lower than that in OPC even from as early as 7 days for the same total chloride content and for a given chloride content and exposure period, the steel reinforcement in the PFA concrete showed lower corrosion current and less negative potential as compared to that in OPC concrete. For external chloride ingress, the inclusion of PFA prolonged the time to corrosion initiation but there was no significant difference in the quantity of chlorides causing this delay in corrosion initiation between OPC and PFA concrete.

For external chloride ingress, the corrosion current density continued to increase in OPC till the end of test period of 12 months whereas in PFA concrete the corrosion current density tended to level off between 3 and 4 months with only nominal increase thereafter. The comparison of the gravimetric weight loss measurements with the degree of corrosion calculated from the linear polarization test showed that the line of equality supports the selection of the vale of B (Stern-Geary constant) equal to 26mV used for determination of corrosion current density. Further the authors observed that higher levels of corrosion occurred in admixed chloride specimens than those exposed to external chloride although the results from the two chloride exposures were obtained at slightly different ages. In addition the results indicated that the concrete grade, curing are the other important factors influencing the degree of corrosion at a given level of chloride contamination.

Baweja et al. (1998) have carried out an experimental investigation by measuring corrosion current by potentiodynamic anodic polarization technique and calculated the area under the corrosion current versus time of exposure envelope as A_{cr} (corrosion activity). The authors also measured concrete resistivity and the gravimetric mass losses of steel in reinforced concrete slabs made with a high-C_3A ordinary Portland cement, a low-C_3A ordinary Portland cement, slag-blended cement and a fly-ash blended cement. The specimens were prepared with varying water-binder ratios (w/b) and were exposed to condition of partial immersion in 3% sodium chloride solution for a period of about 5 years. It was observed that the values of corrosion current were higher for reinforcement in concrete slabs made with higher water-binder ratios than those made with lower water-binder ratios and were lower for the steel reinforcement in concrete slabs made with blended cements than those in OPC at the same w/b ratio. The water-binder ratio significantly influenced the values of A_{cr} for the steel reinforcement with lower values at lower w/b ratio. Binder type also influenced the A_{cr} values but not to the same extent as w/b ratio. Lower values of A_{cr} were observed in concrete slabs made with blended cements than OPC. The parameters i.e. corrosion current and A_{cr} correlated well with the corroded area of the steel reinforcement and gravimetric weight loss data. Approximately after 5 years of exposure to chlorides, steel mass loss increased with the increase in w/b ratio. The blended cement concretes had high resistivitiy characteristics as compared to ordinary Portland cement concrete. The results indicated that, the blended cement concretes

with low water to binder ratio were found to have higher resistivity characteristics, lower corrosion characteristics, and lower reinforcement mass losses when compared with the equivalent Portland cement concretes.

Page et al. (1986) have conducted an experimental investigation to rank different types of cement such as OPC with different C_3A contents, sulfate resisting Portland cement (SRPC), slag blended cement and fly ash blended cement by measuring [Cl^-/OH^-] ratio, chloride diffusivity and assessing the validation of the predicted rank orders by determining the corrosion rate of the embedded steel electrodes in cement paste samples admixed with sodium chloride. From the results, it was found that SRPC offered poorest performance than other cements while the blended cements were at least as effective as the OPC in their ability to protect steel reinforcement from chloride induced corrosion.

Mangat and Molloy (1991) have conducted out an experimental investigation to compare the performance of different concrete matrices made with OPC and OPC with varying replacements levels of PFA, ground granulated blast furnace slag (GGBFS) and microsilica at a constant water cementitious ratio of 0.58. For this purpose they have measured the corrosion potentials and polarization resistances of prism specimens made with above binders and 12mm diameter deformed high yield steel reinforcing bars at regular intervals. The specimens were exposed to simulated marine splash zone exposure for about 600 days. In addition some of the specimens were visually observed for corrosion assessment. From the results they observed that the maximum protection against rebar corrosion is provided at 60% replacement of cement by GGBFS and at 10% and 15% replacements by microsilica. In addition they found that the replacement of cement by 15% PFA has no significant effect on corrosion rate of rebar and the corrosion rate increased at higher PFA contents after long term exposure. They observed that the chloride concentration gives a more reliable indication of corrosion activity than Cl^-/OH^-, especially when comparing concretes with different type and contents of replacement (pozzolanic) materials.

Arya and Xu (1995) have investigated chloride binding and its effect on the corrosion rate of rebar by measuring the galvanic current in macro corrosion cells formed by embedding mild steel bars in two layers of concrete made with OPC and alternative cementitious materials such as PFA, GGBS and silica fume (SF) and admixed with

sodium chloride as internal chloride. From the results it was observed that the chloride binding occurred in the decreasing order of GGBS+OPC followed by PFA+OPC, OPC, and SF+OPC. At 1% chloride introduced at the time of mixing, the corrosion rate was found to be more in PFA, silica fume, and GGBS concrete than that in OPC and at 3% chloride dosage GGBS and SF concrete performed better than OPC and PFA concrete.

Hansson et al. (2006) have carried out an experimental investigation to determine the influence of concrete type and properties on microcell and macrocell corrosion rates of steel embedded in concrete. For this purpose they have determined the macrocell and microcell corrosion rate of the steel reinforcement in ASTM G 109 specimens. The specimens were prepared from ordinary Portland cement concrete (OPCC) mixture and two high performance concrete (HPC) mixtures made with slag and fly ash and with black steel as reinforcement. In addition some cylinders were prepared for compressive strength test and rapid chloride permeability test. The ASTM G 109 specimens were monitored for 180 weeks of exposure. The macrocell corrosion rate was determined from the macrocell corrosion current between top bar and bottom bars while the microcell corrosion rate of the top steel bar was determined by linear polarization technique. From the results they concluded that microcell corrosion is the major mechanism of corrosion of steel in concrete. In ordinary Portland cement concrete the microcell and macrocell corrosion rates of the steel reinforcement are of the same order whereas in HPC mixtures the macrocell corrosion rate of the steel reinforcement was negligible and the corrosion was limited to microcell corrosion of the top steel. This is due to the high resistance to ionic flow in HPC mixture than that in OPCC. They found that the microcell corrosion rate in HPC mixtures was lower by approximately one order of magnitude than that in OPCC mixture and this may be due to lower chloride level at top steel bar in HPC than that in OPCC. In addition from the visual observation, they found that there was greater susceptibility of corrosion of steel in OPCC than that in both HPC mixtures.

Soleymani and Ismail (2004) have carried out an experimental investigation to assess the corrosion activity of the steel reinforcement in OPC concrete and high performance concrete specimens made with OPC and silica fume using four corrosion testing techniques namely Tafel plot (TP) technique, Linear polarisation resistance (LPR) technique, half-cell potential (HCP) measurement and chloride content in

concrete. The steel bar complying ASTM A615 was used as steel reinforcement. From the results the authors observed that high performance concrete specimens showed lower corrosion activity levels as compared to OPC concrete specimens.

Miranda et al. (2005) have measured corrosion potential (E_{corr}), polarization resistance (R_p) values and response to short-term anodic current pulses (galvanostatic pulse technique) of steel bars embedded in prisms made with Portland cement mortar and two activated fly ash mortars. One fly ash mortar is activated by sodium hydroxide and the second one by both sodium hydroxide and waterglass (sodium silicate). In addition some of the specimens in each mortar were admixed with 2% (by weight of binder) of chloride in the form of $CaCl_2$ during preparation. They found that activated fly ash mortars in absence of chlorides passivate the steel reinforcement rapidly and effectively as Portland cement mortars with corrosion rate values lower than $0.1\mu A/cm^2$. However addition of 2% Cl^- hindered the passivation in both Portland and fly ash mortars resulting in increase in corrosion rate values approximately 100 times higher than for chloride free mortars. In the absence of chlorides the corrosion potential values varied from -100mV to -200mV (with reference to saturated calomel electrode) in both Portland and fly ash mortars whereas in the presence of chlorides the corrosion potentials values were more negative in fly ash mortars than Portland cement mortars (i.e. -600mV compared to -300mV to -400mV). Similarly the attenuation of polarisation caused by galvanostatic pulses was more rapid in chloride contaminated mortars than that in chloride free mortars.

Sakr (2005) has studied the effect of different percentages of C3A on corrosion of steel reinforcement embedded in paste specimens made from five types of cement i.e. Type I (2% C_3A), Type II (6% C_3A), Type III (10% C_3A), Type IV (8% C_3A) and Type V (4% C_3A). The cylindrical cement paste specimens having one centrally embedded steel bar were prepared with different cover thicknesses and immersed in 5% NaCl and 5% $MgSO_4$ solutions. From the results of half-cell potential measurement, impressed voltage method and impressed current method, it was found that chloride ions are more aggressive for steel reinforcement than sulphate ions. For the specimens immersed in 5% NaCl solution, half-cell potential values decreased with reduction in C_3A content and time of active potential increased with increase in C_3A content. In addition for the specimens immersed in chloride solution, the amount of iron dissolved due to corrosion decreased with increase in C_3A content as indicated

by impressed voltage method. For the specimens immersed in 5% $MgSO_4$ solution, corrosion increased when the C_3A percent is higher than 6%, In addition from the results it was found that the active potential time decreased as C_3A percent increased and also the mass loss of the steel reinforcement increased as the C_3A content of cement increased for specimens immersed in sulphate solution. This may be due to the modification of original passive film by sulphate ions and thereby replacing with a thin protective film. From results of impressed current method it was observed that the steel reinforcement took more time to reach passivity when immersed in chloride solution than when immersed sulphate solution. The authors observed that the optimum percentage of C_3A to control corrosion of reinforcing steel both in chloride and sulphate media is 6%. They concluded that the presence of chloride together with sulphate ions reduces the sulphate attack and observed that the cover thickness also effects the steel corrosion.

Dinakar et al. (2007) have studied the corrosion behaviour of steel reinforcement in concrete made with Portland pozzolana cement and Portland blast furnace slag cement vis-a-vis the ordinary Portland cements produced from the same parent clinkers. For this purpose concrete specimens of different grades were prepared with above types of cement and only one type of steel reinforcement. The corrosion performance of the OPC and blended cements were evaluated through the measurement of resistivity, corrosion rate, pH and carbonation. The corrosion rate was measured by potentiodynamic polarization technique for specimens immersed in both normal and sea water. From the results obtained, the authors observed that fly ash and slag blended cement concretes exhibited higher values of resistivity than their corresponding OPC concretes. The corrosion rates of the steel reinforcement in both fly ash and slag cement concrete specimens were much lower than those obtained in the corresponding OPC specimens. Further slag blended cement exhibited lower values of corrosion rate than flay ash blended cement. The pH values of fly ash and slag blended cement concrete were found to be around 12 resulting in no significant lowering compared to OPC. However the carbonation was higher in both blended cements particularly in slag blended cements.

Vedalakshmi et al. (2006) have carried out macrocell corrosion studies to evaluate the long term performance of the steel reinforcement in OPC and blended cements i.e. Portland pozzolana cement and Portland slag cement. The specimen was similar to

that specified in ASTM G109 but dimensions adopted were different. The specimens were prepared with different strength grades using above three types of cement and only one type of steel reinforcement i.e. cold twisted high yield strength deformed bar. Potential and macrocell corrosion current were measured periodically and the corrosion rate was determined by weight loss method. From the results obtained the authors observed that the blended cements exhibited lower corrosion rates than those exhibited by OPC. The half-cell potential values of rebar embedded in blended cements were less negative than those in OPC. There was reduction in free chloride content in blended cements than OPC. This reduction was due to the pore filling effect by pozzolanic reaction that causes reduction in chloride ion penetration and higher chloride binding in blended cements than that in OPC. However there was reduction in alkalinity in blended cement concretes than OPC concrete and this reduction in alkalinity did not accelerate the corrosion rate of steel bar in blended cements even in presence of higher chloride content.

Ismail and Ohstu (2006) have carried out an experimental investigation to determine the corrosion rate of steel reinforcement in OPC and high performance concrete (HPC) with silica fume using AC impedance technique. The steel bar meeting the specification of ASTM A615 was used as the steel reinforcement. The cylindrical specimens with a centrally embedded steel bar were exposed to NaCl solution of 0%, 1%, 3% and 5% concentrations. In addition the specimens were also subjected to preconditions and cycles of drying and wetting. They have used different types of electrical equivalent circuits for interpreting the AC impedance spectra. From the results they observed that HPC specimens showed lower corrosion rate than OPC specimens. The corrosion rate increased with increase in NaCl concentration. In addition it was observed that higher drying temperature accelerated the corrosion rate significantly both in OPC and HPC.

Choi et al. (2006) have done an experimental investigation to study the corrosion behaviour of steel reinforcement embedded in fly ash concrete and controlled concrete made with various water-binder ratios and completely immersed in 3.5wt. % NaCl solution. The open-circuit potential and electrochemical impedance spectroscopy measurements were carried out at different intervals of immersion to evaluate the corrosion performance. In addition the authors also carried out chloride ion penetration test as per ASTM C1202 to estimate concrete resistance to penetration

of chloride ions. From the results the authors observed that after 30 days of immersion, the potentials of all the specimens became more negative than -273mV(SCE) i.e. potential corresponding 90% probability of occurrence of corrosion and fluctuated and this may be due to the polarization phenomena induced by limited oxygen diffusion. The partial replacement with fly ash resulted in increase in corrosion resistance and reduction of corrosion rate due to the decrease in permeability of chloride ions. In addition the authors found that concrete resistance increased with decrease in water-binder ratio.

3.5.2 Effect of other factors- water-cement ratio and grade of concrete

Some works have been carried out by researchers in past to see the effect of water-cement ratio and grade of concrete on chloride induced corrosion. According to *Oh et al. (2003)* the extent of corroded area decreased with decrease in water-binder ratio and the free chloride content increased with the increase in water-binder ratio for the same total chloride addition. *Baweja et al. (1999)* observed that, water-binder ratio highly influenced the corrosion rate of the steel reinforcement in slab specimens partially immersed in 3% sodium chloride solution and they found that, decrease in water-binder ratio resulted in lowering of the gravimetric weigh loss of steel reinforcement in Portland cement concrete and blended cement concretes. *Chalee et al. (2007)* observed through experimental investigation that the decrease in water to cementitious materials ratio could reduce the cover depth required for initial corrosion. They observed that fly ash concretes made with 35% and 50% replacements of fly ash and water to cementitious materials ratio of 0.65 provided better corrosion resistance at 4 year exposure compared to the control concrete made with water to cementitious materials ratio of 0.45. *Vedalakshmi et al. (2006)* stated that, the reduction in corrosion rate in blended cement concretes was more pronounced in 20MPa and 30MPa concretes whereas the reduction was not significant in 40MPa concrete when compared to OPC concrete. *Dhir et al. (1994)* observed that the chloride threshold level corresponding to corrosion current density value of $0.2\mu A/cm^2$ at which the corrosion is assumed to occur increased with increase in grade of concrete. *Gu et al. (2000)* found that no significant corrosion occurred in the slag, silica fume, and controlled Portland cement concrete with water-cementitious ratio of 0.32 after 6 months of ponding with 3.4% sodium chloride solution. However significant corrosion rates were observed for the reinforcing steel embedded in control

Portland cement concrete with water-cementitious material ratio greater than 0.43. The poorest performance was observed for reinforcing steel embedded in control concrete specimens with w/c ratio of 0.76, where the corrosion of the steel was detected even with a concrete cover of 51mm.

3.6 LITERATURE ON GENETIC PROGRAMMING

Gandomi et al. (2010) proposed the formulation of compressive strength of carbon fibre reinforced plastic (CFRP) confined cylinders using Linear Genetic Programming (LGP). The LGP-based models were constructed using two different sets of input data. The first set of inputs comprised of diameter of concrete cylinder, unconfined concrete strength, tensile strength of CFRP laminate and total thickness of utilized CFRP layers. The second set included unconfined concrete strength and ultimate confinement pressure which were the most widely used parameters in the CFRP confinement existing models. The models were developed based on experimental results collected from the available literature. The results demonstrated that the LGP-based formulas predicted the ultimate compressive strength of concrete cylinders with an acceptable level of accuracy. The LGP results were also compared with several CFRP confinement models presented in the literature and found to be more accurate in nearly all of the cases.

Saridemir (2010) developed two models in gene expression programming (GEP) approach for predicting compressive strength of concretes containing rice husk ash at the age of 1, 3, 7, 14, 28, 56 and 90days. For purpose of building the models, experimental results for 188 specimens produced with 41 different mixture proportions were obtained from the literature. According to these experimental results, the models were arranged by using seven different input variables in GEP approach. In according to these input variables, the compressive strength values from mechanical properties of concretes containing rice husk ash were predicted in GEP approach models. The results of training, testing and validation sets of the models were compared with experimental results. All of the results showed that GEP is a strong technique for the prediction of compressive strength values of concretes containing rice husk ash.

Muduli et al. (2013) examined the potential of multi-gene genetic programming (MGGP) based classification approach to evaluate liquefaction potential of soil in

terms liquefaction index (*LI*) using a large database from post liquefaction cone penetration test (CPT) measurements and field manifestations. The database consisted of CPT measurements; cone tip resistance (q_c), friction ratio (R_f), vertical total stress (σ_v) and vertical effective stress of soil ($\sigma_{v}{}'$), seismic parameters; peak horizontal ground surface acceleration (a_{max}) and earthquake moment magnitude (M_w), and the depth under consideration (z). The MGGP models were developed for predicting occurrence and non-occurrence of liquefaction on basis of combination of above input parameters. The performance of the models was found to be more efficient compared to available artificial neural network models.

3.7 CLOSING REMARKS

In this chapter literature on effect of cement type, water- cement ratio, grade of concrete on corrosion and genetic programming is discussed

CHAPTER 4 EXPERIMENTAL INVESTIGATION

4.1 GENERAL

Corrosion initiation takes place when the chloride concentration at the rebar level reaches a critical value. As evaluated in chapter 2 the critical chloride level to develop active corrosion of the steel reinforcement is not a unique value. The main reason for uncertainity about this critical chloride level, which is also often referred as threshold chloride concentration, is its dependency on large number of variables. The determining parameter indicating corrosion initiation shall account for steel surface condition and/ or steel type in addition to accounting for the concrete characteristics and chloride ion concentration. Thus pure chemical indicators such as critical levels of free chloride, total chloride or [Cl^-/OH^-] ratio may not be adequate for indication of rebar corrosion initiation against chloride induced corrosion. Electrochemical indicators on the other hand may account for both steel as well electrolytic condition of concrete. The values of corrosion current density, a determining parameter for indication of corrosion initiation obtained by different techniques vary from each other. In addition the corrosion rates obtained by different corrosion monitoring equipments also do not agree with each other. On the other hand half-cell potential value is measured with reference to a standard reference electrode, and depends on the steel type and the electrolytic environment of concrete surrounding. The method of measurement is based on a simple technique and well established equivalence is available for converting the potential obtained from one reference electrode to another. Thus half-cell potential can serve as a determining parameter for indicating initiation of corrosion. For this purpose in this chapter an attempt has been made to experimentally demonstrate the suitability of half-cell potential as a determining parameter for indicating rebar corrosion initiation and to study the effect of different types of steel and cement on the same.

4.2 EXPERIMENTAL DETAILS

The experimental program showing details about the materials, chloride exposure and different tests for corrosion initiation performance is shown in Fig. 4.1.

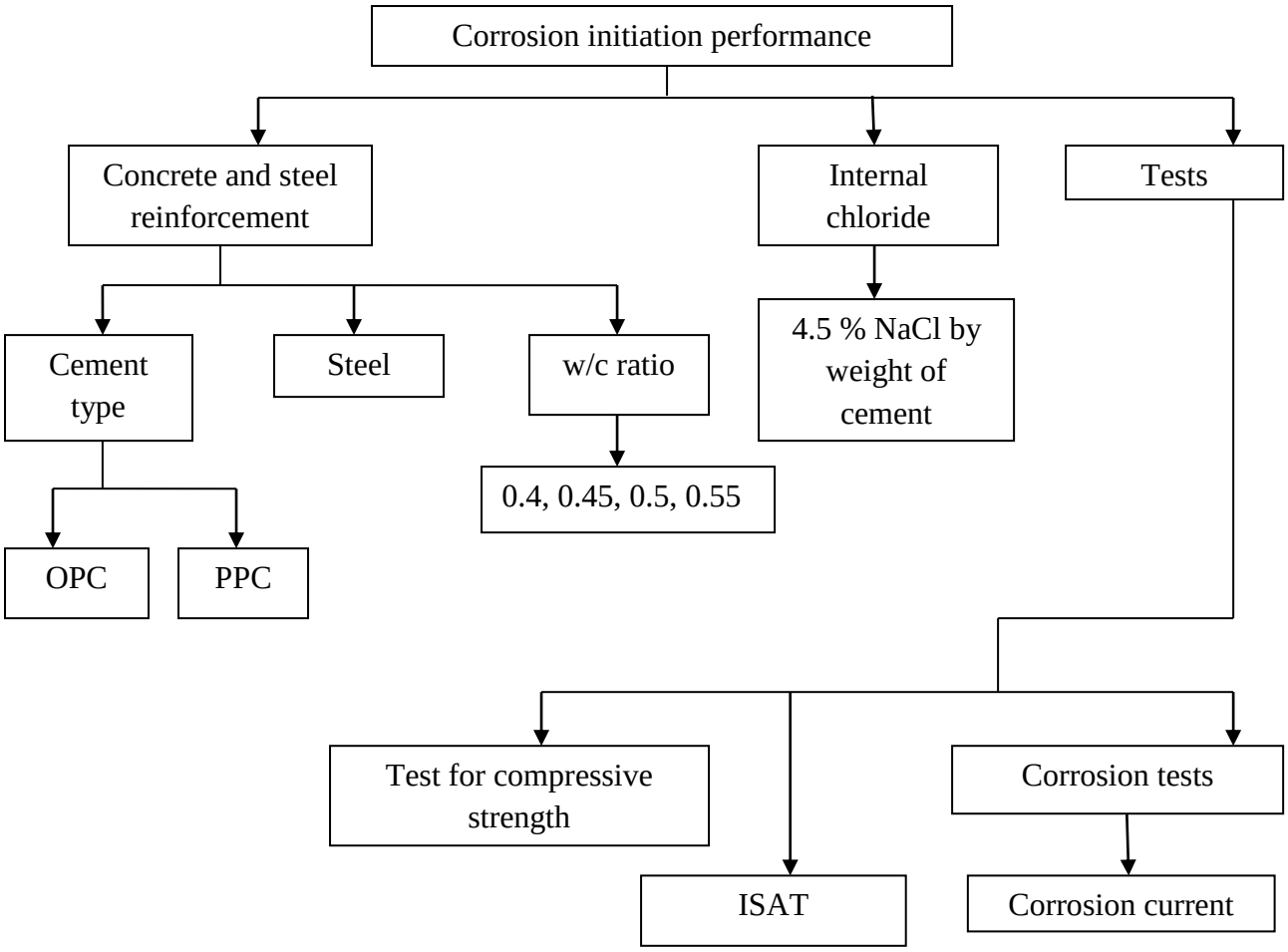

Fig. 4.1: Experimental details for corrosion performance

4.3 MATERIALS

The main test variables for the experimental investigation include cement type, and w/c ratio.

4.3.1 Cement

The following two types of cements which are most commonly used in RC structures were used in the experimental investigation.

1) Ordinary portland cement (OPC) satisfying Indian standards IS: 8112-1989.

2) Portland pozzolana cement (PPC) having 20% pozzolana (fly ash) content, satisfying Indian standards IS: 1489 (Part I) – 1991.

The chemical of the two types of cement as obtained from the manufacture are presented in Table 4.1. The physical tests on both cements i.e. OPC and PPC were conducted in the laboratory and their results are represented in Table 4.2.

Table 4.1: Chemical composition of cements

Compound	OPC	PPC
CaO (%)	62.1	47.72
SiO_2 (%)	21.14	28.82
Al_2O_3 (%)	5.23	9.31
Fe_2O_3 (%)	4.42	4.6
MgO (%)	1.14	1.48
SO_3 (%)	2.3	2.1
LOI (%)	1.5	2.7

Table 4.2: Physical properties of cements

Properties	Results	
	OPC	PPC
Compressive strength (N/mm^2)		
3 Day	11.3	10.7
7 Day	20.2	17.3
28 Day	44.2	43.1
Setting time (min)		
Initial	48	51
Final	165	205
Specific gravity	3.15	2.97
Consistency %	28.00	34.00
Fineness %	84.2	85.4

4.3.2 Coarse aggregates

Coarse aggregates of size 20mm and 10mm of quartzite origin were used in the ratio of 1.78:1 to satisfy the overall grading requirement of coarse aggregate satisfying

Indian standards IS: 383-1970. The grading of 20mm and 10mm in the above proportion is presented in Table 4.3 and Table 4.4. The specific gravities of 20mm and 10mm were found to be 2.68 and 2.64.

Table 4.3: Gradation of 20 mm aggregates

Sr.No.	Sieve Size (mm)	Percentage weight retained	Percentage passing	Cumulative percentage retained
1	80	0	100.00	0.00
2	40	0	100.00	0.00
3	20	0.055	98.15	1.83
4	10	2.895	1.72	98.26
5	4.75	0.041	0.36	99.62
6	2.36	0	0.00	100
7	1.18	0	0.00	100
8	600	0	0.00	100
9	300	0	0.00	100
10	150	0	0.00	100
11	PAN	0.011	-	
			SUM	199.69

$$\text{Fineness modulus of coarse aggregates} = \frac{\Sigma C + 500}{100}$$

$$= \frac{199.69+500}{100}$$

$$= 6.99$$

Table 4.4: Gradation of 10 mm aggregates

Sr.No	Sieve size (mm)	Material retained	Percentage retained	Percentage passing	Cumulative percentage retained
1	80	0.00	0.00	100.00	0.00
2	40	0.00	0.00	100.00	0.00
3	20	0.005	0.249	99.73	0.249
4	10	0.485	24.23	75.5	24.479
5	4.75	1.25	62.46	13.04	86.93
6	2.36	0.00	0.00	0.00	100
7	1.18	0.00	0.00	0.00	100
8	600	0.00	0.00	0.00	100
9	300	0.00	0.00	0.00	100
10	150	0.00	0.00	0.00	100
11	PAN	0.261	13.04	-	-
				SUM	111.658

$$\text{Fineness modulus of coarse aggregates} = \frac{\Sigma C + 500}{100}$$

$$= \frac{500 + 111.658}{100}$$

$$= 6.11$$

4.3.3 Fine aggregates

The material which passes through 4.75 mm sieve is termed as fine aggregate. Usually natural sand is used as a fine aggregate at places where natural sand is not available crushed stone is used as a fine aggregate. The sand used for the experimental works procured and conformed to grading zone II. The sieve analysis of fine aggregates is shown in Table 4.5. The physical properties are provided in Table 4.6.

Table 4.5: Gradation of fine aggregates

Sieve size (mm)	Material retained	Percentage retained	Percentage passing	Cumulative percentage
80	0	0.00	100.00	0.00
40	0	0.00	100.00	0.00
20	0	0.00	100.00	0.00
10	0	0.00	100.00	0.00
4.75	5	0.50	99.50	0.50
2.36	59	5.90	93.60	6.40
1.18	136	13.60	80.00	20.00
600	**243**	**24.30**	**55.70**	**44.30**
300	415	41.50	14.20	85.80
150	122	12.20	2.00	98.00
PAN	20	2.00		
SUM	1000		SUM	255.00

$$\text{Fineness modulus of coarse aggregates} = \frac{\Sigma C + 500}{100}$$

Fineness modulus of aggregates = 2.55

Table 4.6: Physical properties of fine aggregates

Sr. No.	Characteristics	Value
1.	Type	Natural sand
2.	Specific Gravity	2.58
3.	Fineness Modulus	2.55
4.	Grading Zone	Type III

4.3.4 Mixing water

Tap water from laboratory of deep ground water source was used in the experimental work.

4.3.5 Steel

Thermo- mechanically treated (TMT) bars are generally used these days as steel reinforcement in the construction of RC structures. Thus TMT bar is used for experimental investigation. The diameter of the steel bars used was 20mm.

4.3.6 Admixture

Conplast SP430, the admixture supplied by Fosroc India Pvt. Limited is used in our investigations. It is a highly effective superplasticizer for concreteand mortar. It meets the requirements for superplasticizer according to BS 5075 Part 3, ASTM C-494Type A and Type F and IS: 9103-1999 (amended 2003). The dosage of the superplasticizer is fixed based on the requirements for workability. The technical data related to the superplasticizer used is provided in Table 4.7. This data is supplied by the manufacturers.

Table 4.7: Technical data of admixture

Sr. No.	Characteristics	Value
1.	Colour	Brown
2.	Specific gravity	1.20
3.	Air entrainment	Minimum 1%
4.	pH	7 to 8

4.4 CONCRETE MIX PROPORTION

As per Indian standards IS 456-2000 for reinforced concrete of normal strength grade, the maximum free water-cement ratio for mild, moderate, and severe conditions are 0.55, 0.50, 0.45 respectively. Therefore considering the normal strength concrete mixes with above exposure conditions, w/c ratios of 0.4, 0.45, 0.50, 0.55 were selected. All the concrete mixes have been designed for similar workability with slump of 50-80mm. Water content was kept constant to 160 Kg/m^3. A number of trial tests were conducted to get the desired slump with different amount of super plasticizer (SP). To vary the strength, w/c ratio was varied by changing the cement content. The w/c ratio, cement, fine aggregate content and coarse aggregate content

mixes with two types of cement are presented in Table 4.8. Conplast SP 430 was used as super plasticizer for obtaining desired slump.

Table 4.8: Concrete mix proportion

Cement type	Water/ cement ratio	Cement content, (C) (Kg/m^3)	Fine aggregate content, (Kg/m^3)	Coarse aggregate content(20mm), (Kg/m^3)	Coarse aggregates content(10mm) , (Kg/m^3)	SP (%) of C
OPC	0.40	400.00	822.65	523.20	519.27	1.0
	0.45	355.55	813.99	557.09	552.90	0.8
	0.50	320.00	862.32	548.44	544.31	-
	0.55	290.90	691.15	646.64	641.78	-
PPC	0.40	400.00	822.65	523.20	519.27	1.0
	0.45	355.55	805.93	551.57	547.43	0.8
	0.50	320.00	854.15	543.24	539.24	-
	0.55	290.90	691.15	646.64	641.78	-

4.5 PREPARATION OF SPECIMENS

In this section casting procedure for compressive strength test, Initial surface absorption test and corrosion were discussed.

4.5.1 Specimens for compressive strength and ISAT

With two type of cement, four water- cement ratio, one admixed chloride, three replicates, total 48 number of cubes of size 150mm x150mm x150mm were prepared and demoulded. The cubes were then moist in a curing tank for 27 days after demoulding. For casting, the entire test specimen were cleaned and oiled properly. These were securely tightened to correct dimensions before casting. Care was taken that there is no gaps left from where there is any possibility of leakage of slurry.

4.5.2 Preparation and preconditioning of steel specimens

The embedded steel specimens in concrete beam were prepared in a manner similar to that mentioned in ASTM G 109. The steel specimens were cut to the required length of 360mm. These specimens were drilled and threaded at one end to be fitted with the coarse threaded stainless steel screws and nuts. They were then rubbed by wire brush to remove any rust present on the surface and cleaned by soaking in analytical reagent grade hexane. After that the reinforcing steel specimens were allowed to air dry. One stainless steel screw and two nuts were attached to the drilled and threaded end of each of the cleaned steel specimen. The line diagram of the steel specimen is shown in Fig. 4.2. Insulating tape was applied on each end of the steel bar, so that the central 200mm portion of the bar is bare. 3mm thick neoprene tube with internal diameter 20mm was mounted over the insulating tape for a length of 90mm at each end of the steel bar. Epoxy was then filled in the length of the neoprene tube extending from the ends of the steel specimens and also applied at the inner end of the neoprene tube over the steel bar.

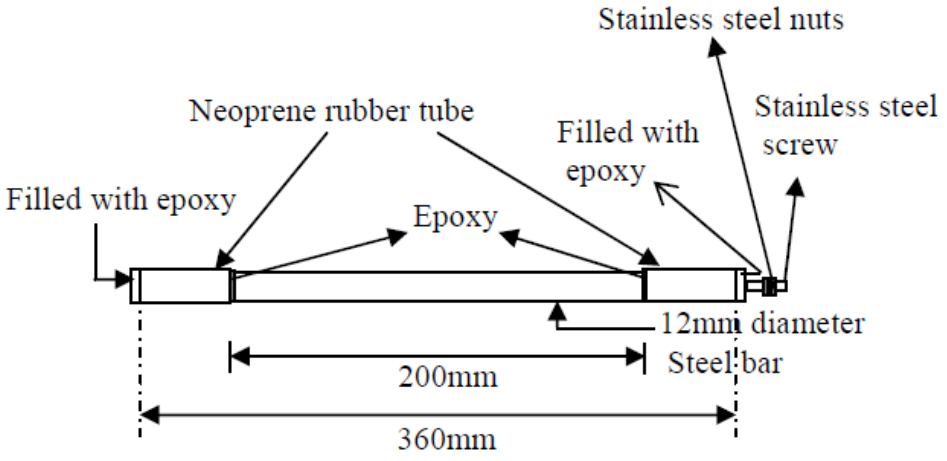

Fig. 4.2: Line diagram of steel specimen

4.5.3 Preparation of slab specimens

The slab specimens prepared were size of 300mm x 300mm x 52m, having a centrally embedded steel specimen mentioned in previous section. A line diagram of slab specimen with its dimensions is shown in fig. 4.3. The cover of reinforcement bar is

16mm. The slab specimens were demoulded after 24hours of preparations and were moist cured for 27days in a curing tank. On completion of moist curing, the slab specimens were kept in the ambient laboratory conditions till testing shown in fig.4.4. With two type of cements, four water cement ratio, one admixed chloride content and one replicates, total of 8 slabs specimens were prepared. Linear polarization resistance test was conducted on all slab specimens at the age of 60 days. For casting, the entire test specimen were cleaned and oiled properly. These were securely tightened to correct dimensions before casting. Care was taken that there is no gaps left from where there is any possibility of leakage of slurry.

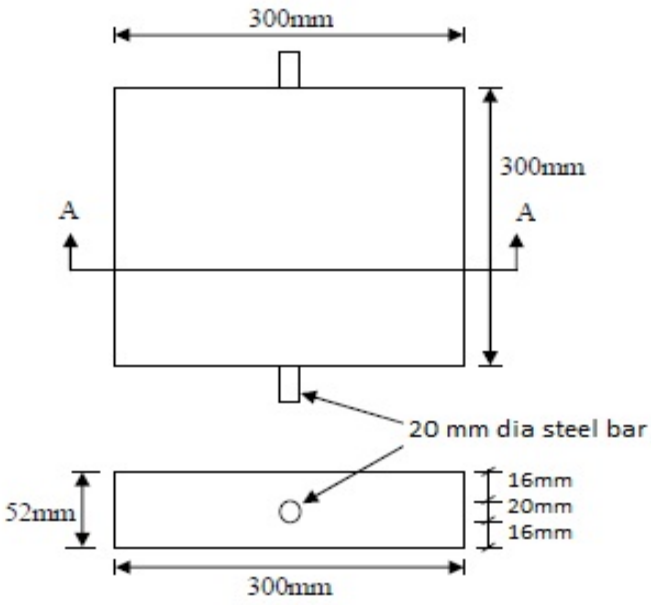

Fig. 4.3: Line diagram of slab specimen

Fig.4.4: Slab specimens in laboratory

4.6 TESTING OF SPECIMENS

In this section test setup for the tests (compressive strength test, initial surface absorption test, rebar corrosion) are discussed.

4.6.1 Initial surface absorption test

BS 1881: PART 208:1996 gives recommendations for a method of determining the initial surface absorption of oven dried concrete, of concrete in the laboratory which cannot be oven dried on site. ISAT is qualitative test, however in the present research programme, it is used along with compressive strength results to get quantitative measure of rebar corrosion.

Assembling the apparatus

Set up the reservoir so that when it is filled a head of 180 mm to 220 mm of water is applied to the surface of the concrete.

Connect the reservoir to inlet of the cap with the flexible tube, which has the top fitted to it.

Starting of the test

Measure and report the temperature of the concrete surface adjacent to the cap to the nearest 1°C. Close the tap from the reservoir and fill the reservoir with water. Start the test by opening the tap to allow the water to run into the cap and record this start time. Flush all the air from the cap through the capillary tube, assisted if necessary, by sharply pinching the flexible tubing. Replenish the reservoir to maintain the head of 180 mm to 220 mm of water and raise on end of the capillary tube just above the water level to prevent further overflow. Take care at all times to ensure that the reservoir does not empty itself.

Readings

Take readings normally after the following intervals from the start of the test:

- 10mins
- 30 min
- 1 hour
- 2 hour

As the test proceeds, the moisture content of the concrete will increase and capillary pores within the concrete adjacent to the test area become water filled. The rate of surface absorption will normally diminish as the duration of the test increases. Just before the specified intervals lower the capillary tube so that water runs in to fill it completely and then fix it in a horizontal position at the same level as the surface of the water in the reservoir.

At each of the specified test intervals close the tap at allow water to flow back along the capillary tube.When the meniscus reaches the scale start the stop watch. After 5s note the number of scale divisions the meniscus has moved and, by reference to table 4.9, determine the period during which the movement is to be measured.

Table 4.9: Determination of period of movement

Number of scale divisions moved in 5 s	Period during which movement is measured
<3	2 min

3 to 9	1 min
10 to 30	30 s
>30	Record initial surface absorption as more than 3.60 ml/(m^2.s)
Note 1 divisions = 0.01 unit	

Record the number of scale divisions moved during the period selected from table 3.9. When the reading are taken over a 2 min or 30sec period, multiply the number of divisions by 0.5 or 2 respectively to convert the reading to 1 min period. Record the actual or equivalent number of scale units traversed per min, which is 0.01 times the number of divisions, as the initial surface absorption in ml/(m^2.s) for that particular test interval. If the movement over the 5 sec period exceeds 30 scale divisions record the initial surface absorption as more than 3.60 ml/(m^2.s).

If the reading taken 10min after the start of the test is below 0.05 ml/(m^2.s), stop the test with the comment "concrete too impermeable to be sensitive to a longer term test". Similarly, where the 10 min reading is above 3.60 ml/(m^2.s), stop the test and record the result with the comment concrete too permeable to be within the sensitivity of the test method.

Between test intervals leave the tap open and maintain the level of the water in the reservoir at the specified head. The capillary tube may be tilted or raised a little to prevent overflow of the water. General arrangement and setup of ISAT is shown in fig. 4.5 and fig. 4.6.

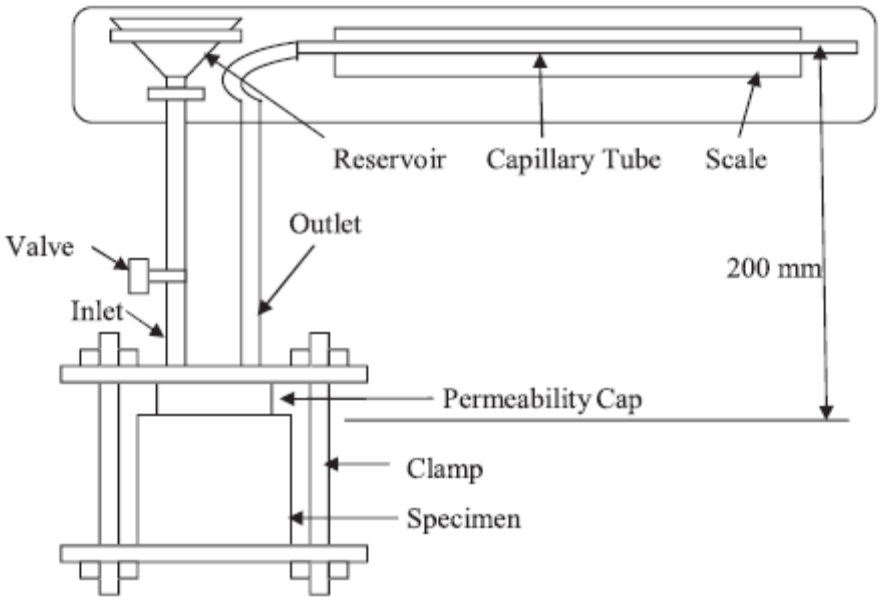

Fig.4.5: General arrangement of ISAT

Fig.4.6: Setup of ISAT

4.6.2 Compressive strength

Three identical specimens are crushed at 28 days. The compressive strength is calculated by dividing the failure load by average cross sectional area. The compressive strength testing machine of capacity 5000 KN is used for determining the maximum compressive loads carried by concrete cubes. The compressive strength test machine which used in all tests is shown in fig.4.7. At the test age the specimens are taken out of the curing tank and kept outside for 10 minutes. Then one specimen is

placed on the steel plate of the machine such that the specimen is tested perpendicular to the casting position. Then the test is carried out at the loading rate of 5 KN/s specified IS: 516- 1959.

Fig.4.7: Testing for compressive strength

4.6.3 Corrosion rate by linear polarization resistance (LPR) technique

Linear polarization resistance test with IR compensation was conducted with guard ring arrangement on all 8 slab specimens of all the concrete mixes at the age of 60

days. As concrete is a high resistive media, the IR drop in the cover concrete is significant and may vary from specimen to specimen. Therefore the IR drop value of the cover concrete needs to be determined and compensated for determining the corrosion current density. The instrument automatically compensates for the above IR drop and also records the IR drop value. For linear polarization resistance measurement, the working electrode i.e. the steel reinforcement in the slab specimen was polarized to ±25mV from the equilibrium potential at a scan rate of 0.1mV per second. The LPR measurement with IR compensation technique used with the corrosion instrument automatically calculates the equivalent IR value of the cover concrete and compensates while determining the corrosion current density. Before performing the test, the conducting sponge was wetted with soap solution and placed on the surface of the slab specimen to have proper electrical contact with the guard ring. Assembly of guard ring electrode, auxiliary electrode and reference electrode was then placed above the wetted sponge. The electrical connections were made to the steel reinforcement. The experimental arrangement for LPR measurement with guard ring arrangement is shown in fig.4.8. The polarized surface area of the steel reinforcement was taken to be that lying under a circle intersecting the midpoint between the two sensor electrodes and only the top half surface area of the steel reinforcement was assumed to be polarized. For calculation of the corrosion current density I_{corr}, Stern-Geary equation was used;

$$I_{corr} = \frac{B}{Rp}$$

Where B is the Stern-Geary constant and is given by $B= (\beta_a x \beta_c)/2.3(\beta_a+\beta_c)$. β_a and β_c are anodic and cathodic Tafel constants respectively. The value of B was taken as 26mV considering steel in active condition. R_p is the polarization resistance.

Fig.4.8: Guard ring arrangement for measuring I_{corr}

4.7 CLOSING REMARKS

The experimental programme described in this chapter includes the significant material properties and specifications of the ingredients of concrete and the testing procedure. The specimen details and the test set-up have been discussed.

CHAPTER 5 RESULTS AND DISCUSSIONS

5.1 GENERAL

In this chapter the parameters studied on the control and concrete admixed with 4.5% NaCl by weight of cement are discussed. The parameters such as Compressive strength, Initial surface absorption, I_{corr} resulted from experimental study are discussed and comparisons between the various mixes are represented. The abbreviation of various mix admixed with 4.5% chloride content of cement are enlisted in table 5.1.

Table 5.1: Abbreviation of various mix

Sr. No.	Cement type	Water-cement ratio	Abbreviation
1	OPC	0.40	A0.40
2	OPC	0.45	A0.45
3	OPC	0.50	A0.50
4	OPC	0.55	A0.55
5	PPC	0.40	B0.40
6	PPC	0.45	B0.45
7	PPC	0.50	B0.50
8	PPC	0.55	B0.55

5.2 COMPRESSIVE STRENGTH

The compressive strength of cubes at the ages of 28 days was determined in compression testing machine and the results for all the cubes prepared from all the concrete mixes respectively at the ages of 28 days. Compressive strength of both mix at different admixed chloride level i.e. at 0% and 4.5% are represented.

Table 5.2: Compressive strength at the age of 28 days

Mix	Compressive strength (N/mm^2) at admixed content		Average compressive strength (N/mm^2) at admixed content	
	0%	4.5%	0%	4.5%
A0.40	52.31	47.64	52.23	47.18
	53.20	48.69		
	51.20	45.23		
A0.45	46.50	41.18	45.32	40.46
	45.60	39.97		
	43.88	40.23		
A0.50	37.23	37.06	36.01	35.71
	36.54	34.62		
	34.26	35.45		
A0.55	32.24	31.70	32.01	31.43
	32.20	30.64		
	31.59	31.96		
B0.40	56.24	48.47	54.41	47.90
	55.67	44.62		
	51.32	50.63		
B0.45	49.50	42.67	47.57	42.47
	47.62	43.39		
	45.60	41.36		
B0.50	41.44	39.44	40.44	39.45
	40.26	38.65		
	39.62	40.25		
B0.55	39.02	37.28	38.17	37.02
	38.79	36.50		
	36.70	37.29		

The comparison of compressive strength at 0% admixed level and 4.5% admixed level are shown in fig. 5.1 and fig.5.2.

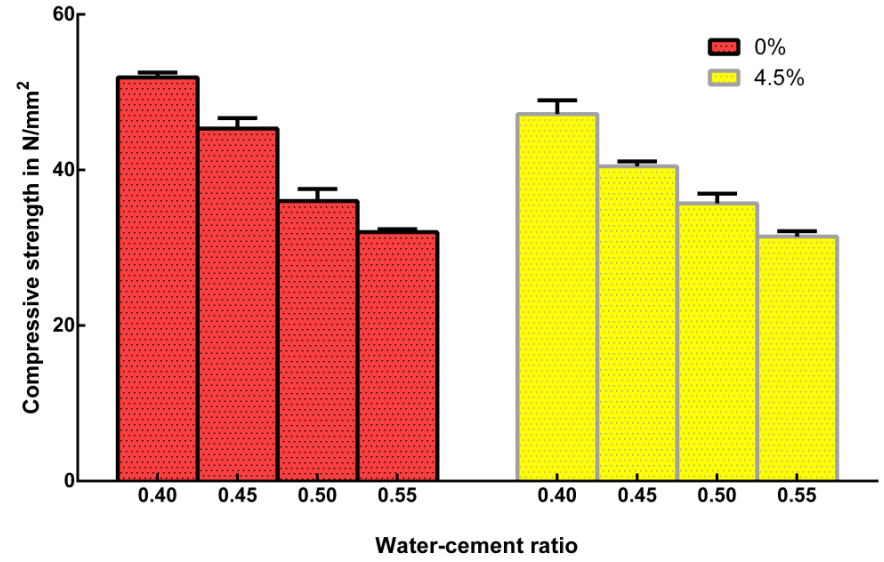

Fig.5.1: Compressive strength at the age of 28 days of A mix.

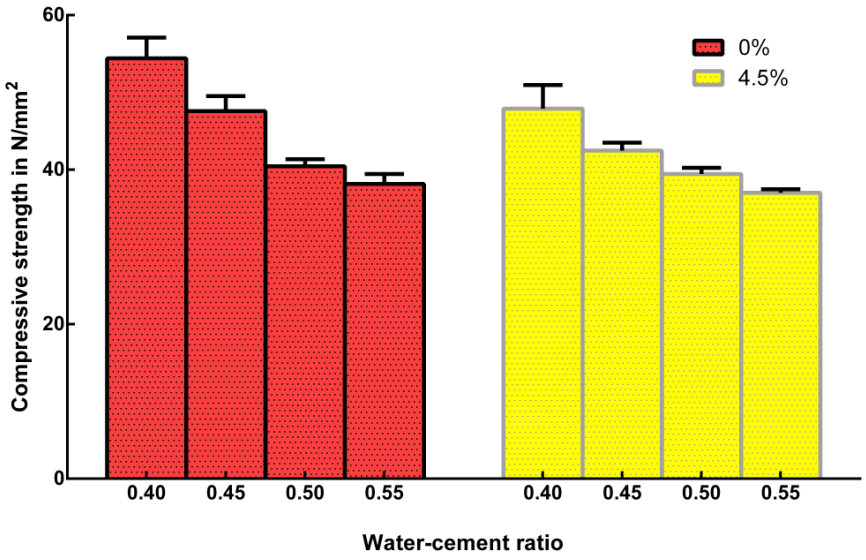

Fig.5.2: Compressive strength at the age of 28 days of B mix

From these fig. 5.1, 5.2 it is observed that the concrete cubes made with PPC exhibited higher compressive strength than those made with OPC. However this increase in compressive strength was more in blended cements i.e. PPC than that in OPC. Chloride level does not significantly affect the compressive strength of concrete at 28 day age. PPC exhibits more value of compressive strength as compared to OPC. This is beacuse pozzolanic action has started before testing which results in more strength.

5.3 INITIAL SURFACE ABSORPTION TEST

The test for initial surface absorption of concrete is a test to indicate the water flow into the surface of a dry, flat concrete surface. The test is time dependant and comparative to indicate the quality of concrete to resist absorption of water. The ISAT is performed to obtain an indication of the durability of concrete subjected to external chemical attack. Results of initial absorption test conducted on various mixes are presented in table 5.3. And their comparison of flow at different intervals i.e. 10min, 30min, 60min, 120min are shown in fig.5.3, 5.4.

Table 5.3: Initial surface absorption results of all mix

Sample type	Time interval (min)	No. of divisions (N)	Flow =0.01x N ($ml/m^2.s$)
A0.40-1	10	62	0.62
	30	54	0.54
	60	53	0.53
	120	50	0.50
A0.40-2	10	129	1.29
	30	105	1.05
	60	59	0.59
	120	39	0.39
A0.40-3	10	79	0.79
	30	65	0.65
	60	53	0.53
	120	41	0.41
A0.45-1	10	90	0.90
	30	76	0.76
	60	62	0.62
	120	56	0.56
A0.45-2	10	150	1.50
	30	120	1.20
	60	97	0.97
	120	65	0.65

A0.45-3	10	72	0.72
	30	53	0.53
	60	51	0.51
	120	14	0.14
A0.50-1	10	105	1.05
	30	89	0.89
	60	74	0.74
	120	52	0.52
A0.50-2	10	97	0.97
	30	73	0.73
	60	54	0.54
	120	34	0.34
A0.50-3	10	90	0.90
	30	72	0.72
	60	59	0.59
	120	43	0.43
A0.55-1	10	60	0.60
	30	45	0.45
	60	33	0.33
	120	29	0.29
A0.55-2	10	120	1.20
	30	87	0.87
	60	81	0.81
	120	54	0.54
A0.55-3	10	89	0.89
	30	75	0.75
	60	64	0.64
	120	51	0.51
B0.40-1	10	85	0.85
	30	71	0.71
	60	63	0.63
	120	41	0.41

B0.40-2	10	79	0.79
	30	69	0.69
	60	52	0.52
	120	39	0.39
B0.40-3	10	85	0.85
	30	74	0.74
	60	57	0.57
	120	43	0.43
B0.45-1	10	69	0.69
	30	59	0.59
	60	51	0.51
	120	42	0.42
B0.45-2	10	49	0.49
	30	34	0.34
	60	25	0.25
	120	20	0.20
B0.45-3	10	69	0.69
	30	54	0.54
	60	47	0.47
	120	39	0.39
B0.50-1	10	171	1.71
	30	107	1.07
	60	89	0.89
	120	56	0.56
B0.50-2	10	80	0.80
	30	67	0.67
	60	54	0.54
	120	32	0.32
B0.50-3	10	120	1.20
	30	95	0.95
	60	72	0.72
	120	59	0.59

B0.55-1	10	67	0.67
	30	59	0.59
	60	42	0.42
	120	32	0.32
B0.55-2	10	93	0.93
	30	77	0.77
	60	54	0.54
	120	46	0.46
B0.55-3	10	89	0.89
	30	72	0.72
	60	49	0.49
	120	41	0.41

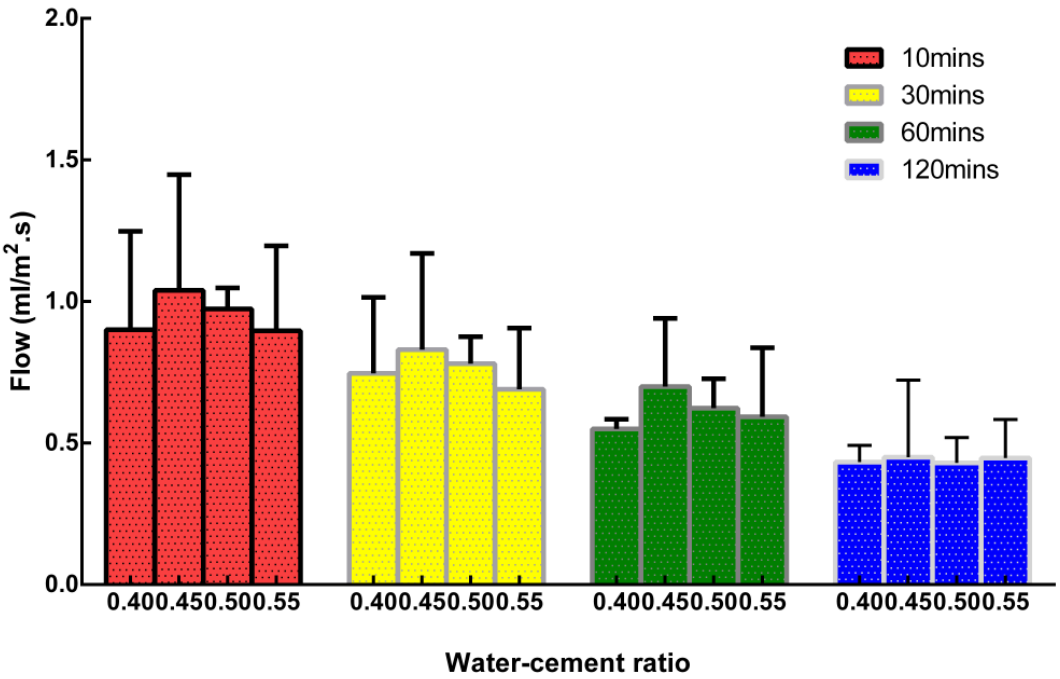

Fig.5.3: ISAT results of A type

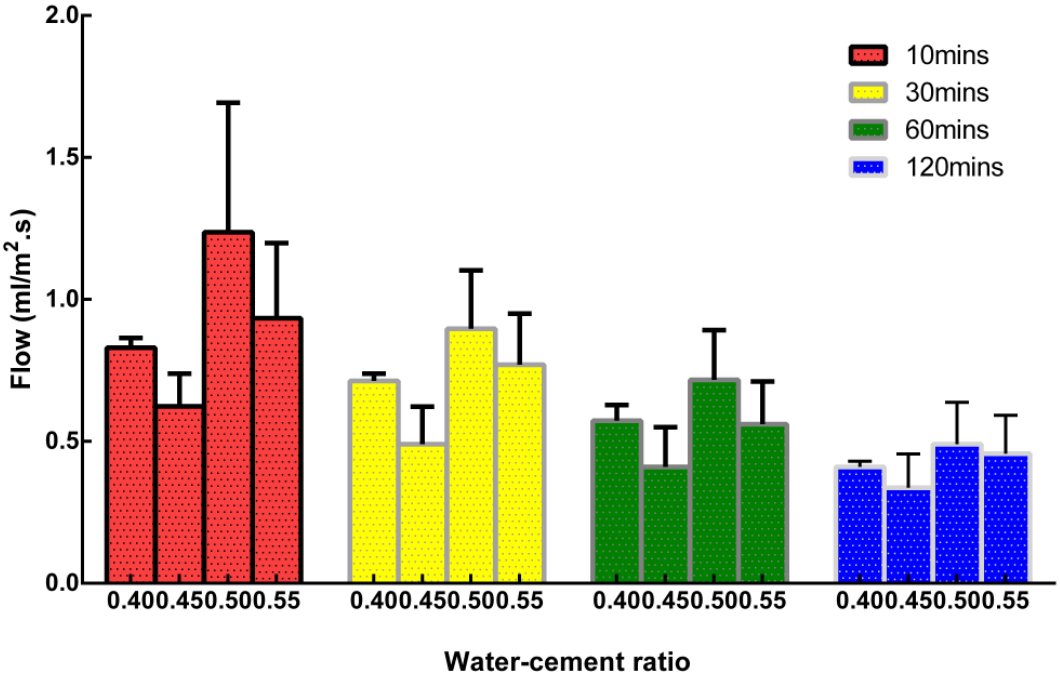

Fig.5.4: ISAT results of B type

It was observed that initially the flow rate was high. But with increasing time, the flow through concrete decreased drastically, becoming constant almost after one hour. Similar trend was visible in each mixture.

5.4 MEASUREMENT OF CORROSION

Corrosion is measured through LPR(linear polarization resistance) i.e. I_{corr}. Long term LPR technique performed on ACM Field machine was used to record Rest Potential (R_p), I_{corr}, E_{corr} and corrosion rate. Tafel extrapolation technique was used for further modification of these results. It is shown in fig. 5.5.

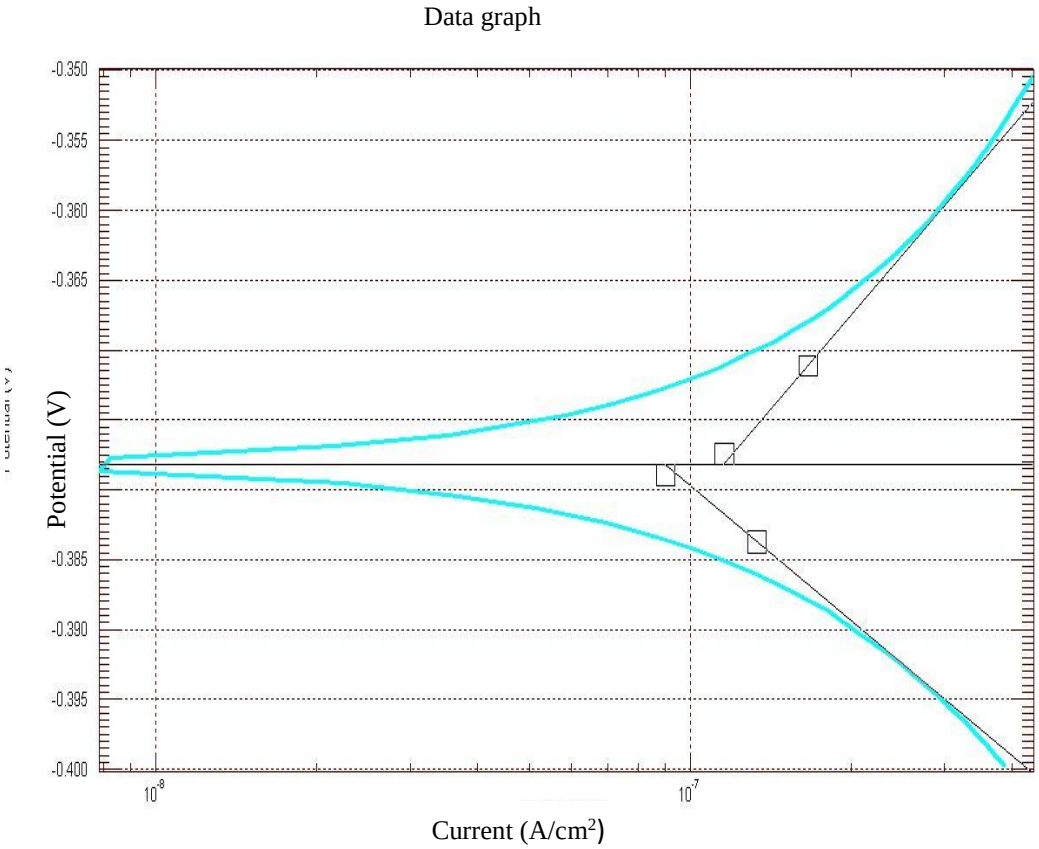

Fig. 5.5: Tafel extrapolation technique

5.4.1 Tafel Plots from ACM Field Machine

Tafel plot gives variation of potential (V) at Y-axis with respect to logarithmic current (log I) at X-axis. Tafel plots give more precise values of I_{corr} and corrosion rate by the use of Tafel extrapolation. Tafel ruler function in sequencer of ACM field machine can be used for Tafel extrapolation. Tafel rulers can only be used on potential vs current graphs where the current axis is logarithmic. Three rulers are placed on the graph, a horizontal ruler which identifies the rest potential. The other rulers indicate Tafel slopes.

The potential curve of the Tafel plot helps us to judge the corrosion potential (E_{corr}) values and the passive behaviour of rebar. Corrosion current density values of various mix are enlisted below in table 5.4. All these values of I_{corr} are taken at 60days.

Table 5.4: Corrosion current density of various mix

Sr.no.	Sample type	I_{corr} (mA/cm^2)
1	A0.40	0.0709
2	A0.45	0.0268
3	A0.50	0.0136
4	A0.55	0.0468
5	B0.40	0.0297
6	B0.45	0.0119
7	B0.50	0.0286
8	B0.55	0.0370

It is observed that variation in corrosion current density is not systematic with water-cement ratio. But corrosion is relatively significant. Corrosion is more in OPC cement as compared to PPC. Thus blended cement performed well as compared to OPC.

5.5 DEVELOPMENT OF MODEL

Initial surface absorption is qualitative test, however in the present research programme it is used as quantitative measure of rebar corrosion. Thus compressive strength and initial surface absorption are independent properties where as rebar corrosion is dependent. Rebar corrosion is dependent on initial surface absorption and compressive strength and there model is developed using GP kernel. Genetic Programming is a technique for the automatic and systematic solving of problems by means of algorithmic evolution, regardless of domain. Following table consist to independent parameters i.e. compressive strength and ISAT. The values of ISAT are average value of three replicates shown in the table 5.5. Data consists of compressive strength which is divided by 100 in this process. Values are different intervals i.e. at 10min, 30min, 60min and 120min are given in input data. Excel sheet is made by all input data and this sheet is saved as .csv fomat. In following table CS represents compressive strength, IS10 represents initial surface absorption at 10min, IS30 represents initial surface absorption at 30min, IS60 represents as initial surface absorption at 60min, IS120 represents initial surface absorption at 120min in ($ml/m^2.s$) and IC represents I_{corr} value in mA/cm^2.

Table 5.5: Input data in GP kernel

Sr. No.	CS	IS10	IS30	IS60	IS120	IC
1	0.5223	0.83	0.71	0.55	0.44	0.0709
2	0.4532	1.04	0.83	0.70	0.45	0.0268
3	0.3601	0.92	0.78	0.63	0.43	0.0136
4	0.3201	0.90	0.69	0.60	0.45	0.0468
5	0.5441	0.83	0.72	0.58	0.41	0.0297
6	0.4757	0.63	0.49	0.41	0.34	0.0119
7	0.4044	1.24	0.90	0.71	0.49	0.0286
8	0.3817	0.83	0.69	0.48	0.40	0.0370

The excel sheet is generated in the .csv format is copied in the gpkernel folder. Various variable parameters are generations, population, child, function and cross over rate. Various trials are made by changing parameters. The function used for the entire process is linear throughout. The cross over rate is 0.4. There are two objectives in this process i.e. Coefficient of determination (COD) and Root mean square (RMS). The value of COD should be nearly one and value of RMS should be nearly zero. For exact result COD should be equal to one and RMS should be zero. Number of alterations are made in gpkernel and final equation is represented (5.1) below with dominant factors affecting corrosion and values of COD and RMS are given in the table 5.6 for the following derived equation.

$$I_{corr} = \frac{(b+ab-x)(x+ab)(2x-b)(2b-a)}{ab(x+b)} \quad (5.1)$$

Where “x” is compressive strength, “a” is IS30 and “b” is IS120.

Table 5.6: Value of objectives

Objectives	Value
COD	0.9738
RMS	0.0048

CHAPTER 6 CONCLUSIONS

- Chloride level does not significantly affect the compressive strength of concrete at 28 day age. PPC exhibits more value of compressive strength as compared to OPC.
- It was observed in ISAT that initially the flow rate was high. But with increasing time, the flow through concrete decreased drastically, becoming constant almost after one hour. Similar trend was visible in each mixture.
- IS30 and IS120 are considered in the model. This is because IS30 represents normalized value and IS120 represents true characteristics of concrete.
- Corrosion depends upon independent parameters i.e. compressive strength, value of initial surface absorption at 30min and initial surface absorption at 120min.

SUGGESTIONS FOR FUTURE WORK

The suggestions for further work have been extended to the following;

1) Extensive work was carried out on normal strength concrete by changing sample size, steel type etc.

2) Compressive strength is bulk concrete property. Therefore CAPO test can be conducted to get the compressive strength of surface. Also ISAT is surface property. Thus correlation can be develop between corrosion and surface properties.

REFERENCES

- Alonso, C., Andrade, C., Castellote, M., and Castro, P. (2000). "Chloride threshold values to depassivate reinforcing bars embedded in a standardized OPC mortar." Cement and Concrete Research, Vol. 30, pp. 1047-1055.
- Arya, C., and Xu, Y. (1995). "Effect of cement type on chloride binding and corrosion of steel in concrete." Cement and Concrete Research, Vol. 25, pp. 893-902.
- Basheer, P. A. M., Gilleece, P. R. V., Long, A. E., and Mc Carter, W. J. (2002). "Monitoring electrical resistance of concretes containing alternative cementitious materials to assess their resistance to chloride penetration." Cement and Concrete Composites, Vol. 24, pp. 437-449.
- Baweja, D., Roper, H., and Sirivivatnanon, V. (1998). "Chloride-induced steel corrosion in concrete: Part 1- Corrosion rates, corrosion activity, and attack areas." ACI Materials Journal, Vol. 95, pp. 207-217.
- Baweja, D., Roper, H., and Sirivivatnanon, V. (1999) "Chloride-induced steel corrosion in concrete: Part 2- Gravimetric and electrochemical comparisons." ACI Materials Journal, Vol. 96, pp. 306-313.
- Bertolini, L., Elsener, B., Pedeferri, P., and Polder, R. (2004). "Corrosion of steel in concrete." Wiley-Vch Verlag Gmbh & Co. Kgaa, Weinheim.
- Bhattacharjee,B. and Ahmad,S.(1995). "A simple arrangement and procedure for insitu measurement of corrosion rate of rebar embedded in concrte."Corrosion Science, Vol. 37, No. 5, pp, 781-791.
- Chalee, W., Teekavanit, M, Kiattikomol, Siripanichgorn, A., and Jaturapitakkul, C. (2007). "Effect of W/C ratio on covering depth of fly ash concrete in marine environment." Construction and Building Materials, Vol. 21, pp. 965-971.
- Choi, Y. S., Kim, J. G., and Lee, K. M. (2006). "Corrosion behavior of steel bar embedded in fly ash concrete." Corrosion Science, Vol. 48, pp. 1733-1745.

- Dhir, R. K., Jones, M. R., and McCarthy, M. J. (1994). "PFA concrete: chloride induced reinforcement corrosion." Magazine of Concrete Research, Vol. 46, pp. 269-277.
- Dinakar, P., Babu, K. G., and Santhanam, M. (2007). "Corrosion behaviour of blended cements in low and medium strength concretes." Cement & Concrete Composites, Vol. 29, pp. 136-145.
- Erdogdu, S., Bremner, T. W., and Kondratova, I. L. (2001). Accelerated testing of plain and epoxy-coated reinforcement in simulated seawater and chloride solutions." Cement and Concrete Research, Vol. 31, pp. 861-867.
- Gandomi, A.H., Alavi, A.H. and Sahab, M.G. (2010), "New formulation for compressive strength of CFRP confined concrete cylinders using linear genetic programming", Journal: Construction and Building Materials, Vol. 43, No.7, 963-983.
- Hansson, C. M., Poursaee, A., and Laurent, A. (2006). "Macrocell and microcell corrosion of steel in ordinary Portland cement and high performance concretes." Cement and Concrete Research, Vol. 36, pp. 2098-2102.
- Hausmann, D. A. (1967). "Steel corrosion in concrete: how does it occur?" Materials Protection, Vol. 6 , pp. 19-23.
- Hussain, S. E., Al-Gahtani, A. S., and Rasheeduzzafar. (1996). "Chloride threshold for corrosion of reinforcement in concrete." ACI Materials Journal, Vol. 94, pp. 534-538.
- Lambert, P., Page, C. L., and Vassie, P. R. W. (1991). "Investigations of reinforcement corrosion. 2. Electrochemical monitoring of steel in chloride contaminated concrete." Materials and Structures, Vol. 24, pp. 351-358.
- Mangat, P, S., and Molloy, B. T. (1991). "Influence of PFA, slag, and microsilica on chloride induced corrosion of reinforcement in concrete." Cement and Concrete Research, Vol. 21, pp. 819-834.
- Miranda, J. M., Fernandez-Jimenez, A., Gonzalez, J. A., and Palomo, A. (2005). "Corrosion resistance in activated fly ash mortars." Cement and Concrete Research, Vol. 35, pp. 1210-1217.
- Muduli, P.K., Das, S.K. (2013), "CPT- Based Seismic Liquefaction Potential Evaluation using Multi-gene Genetic Programming Approach", Indian Geotechnical Journal.

- Oh, B. H., Jang, S. Y., and Shin, Y. S. (2003). “Experimental investigation of the threshold chloride concentration for corrosion initiation in reinforced concrete structures.” Magazine of Concrete Research, Vol. 55, pp. 117-124.
- Saridemir, M. (2010), “Genetic Programming approach for prediction of compressive strength of concretes containing rice husk ash”, Journal: Construction and Building Materials, Vol. 24, No.10, 1911-1919.
- Schiessl, P. (1988). “Corrosion of Steel in Concrete.” Report of the technical committee 60-CSC RILEM, Chapman and Hall, New York.
- Shreir, L. L. (1976). “Corrosion, Vol. 1, metal/environment reactions.” Second ed., Newnes-Butterworths, London.
- Soleymani, H. R., and Ismail, M. E. (2004). “Comparing corrosion measurement methods to assess the corrosion activity of laboratory OPC and HPC concrete specimens.” Cement and Concrete Research, Vol. 34, pp. 2037-2044.
- Thomas, M. (1996). “Chloride thresholds in marine concrete.” Cement and Concrete Research, Vol. 26, pp. 513-519.
- Thomas, M. D. A. (1991). “Marine performance of PFA concrete.” Magazine of Concrete Research, Vol. 43, pp. 171-185.
- Trejo, D. (2002). “Evaluation of the critical chloride threshold and corrosion rate for different steel reinforcement types.” www.mmfxsteel.com/PDF/DRTREJ~8.PDF.
- Trejo, D., and Monteiro, P. J. (2005). “Corrosion performance of conventional (ASTM A615) and low-alloy (ASTM A706) reinforcing bars embedded in concrete and exposed to chloride environments.” Cement and Concrete Research, Vol. 35, pp. 562-571.
- Trejo, D., and Pillai, R. G. (2003). “Accelerated chloride threshold testing: part I-ASTM A615 and A706 reinforcement.” ACI Materials Journal, Vol. 100, pp. 519-527.
- Vedalakshmi, R., Rajagopal, K., and Palaniswamy, N. (2006). “Longterm corrosion performance of rebar embedded in blended cement concrete under macro cell corrosion condition.” Construction and Building Materials, Article in press.